Islamic University of Gaza

Deanery of Higher Studies

Faculty of Science

Department of Chemistry

Synthesis and characterization of lead(II) complexes with some polydentate ligands and their application in lead (II)-selective electrodes

Submitted By

Baha Eldin Khader Ayed Daher

Supervisors

Dr. Salman M. Saadeh
Associate prof. of inorganic Chemistry
Chemistry Department
Faculty of Science
Islamic University - Gaza

Dr. Hazem M. Abu Shawish
Associate prof. of Analytical Chemistry
Chemistry Department
Faculty of Science
Al-Aqsa University - Gaza

A Thesis Submitted in Partial Fulfillment of The Requirements For The Degree of Master of Science in Chemistry Islamic University of Gaza, Palestine.
Department of Chemistry Faculty of Science
Islamic University of Gaza
GAZA-PALESTINE

1432هـ - 2011م

DEDICATION

TO

THE SOUL OF MY FATHER, MOTHER, SISTERS, BROTHER, WIFE,

SONS AND FAMILY.

ACKNOWLEDGEMENTS

I am grateful to Allah for giving me health, strength, peace and courage to finish this study .

I would like to express my deepest appreciation and sincere gratitude to my supervisors especially **Dr. Salman M. Saadeh Dr. Hazem M. Abu-Shawish. In addition, I thank Dr. Hany M. Dalloul, Dr. Nabil M. El-Halabi** for their great and continuous help, encouragement and guidance during the research course .

I also extend my thanks to the Islamic University of Gaza and AL-Aqsa University for making available all needed facilities to complete this research.

I truly appreciate all the time my patient mother, wife, sisters, brother, and wonderful sons for their constant support, who were the source of relief and comfort .

Finally, I would like to thank overall my friends and uncles especially **Raid Eldohder** for their continuous help.

Baha Eldin Kh. Daher

ABSTRACT

New Pb(II) complexes of the general formula PbL_2 where HL = 2-acetylthiophene benzoylhydrazone, 2-acetylfuran benzoylhydrazone, 2-carboxaldehydethiophene benzoylhydrazone and 2-carboxaldehydefuran benzoylhydrazone were synthesized by reaction of lead(II) acetate with the ligands in methanol in lead to ligand ratio of 1: 2. The complexes are insoluble in common organic solvents but soluble in DMF and DMSO. The measured molar conductance values in DMF indicate that, the complexes are non electrolytes in nature. In view of analytical and spectral (IR, UV–vis and NMR) studies, it has been concluded that, all the metal complexes possess octahedral geometry in which the ligand is coordinated to lead(II) through azomethine nitrogen, benzoyl oxygen and thiophene sulfur or furan oxygen atom via deprotonation. These complexes were tested as ionophores for lead(II) determination. $Pb(ATBH)_2$ gave the best response with two plasticizers TEph and DOS, that fully characterized. Their detection limits were 3.9 x 10^{-7} M, 7.9 x 10^{-7} M, concentration ranges 5.9 $\times 10^{-7}$ – 1.0×10^{-2} M, 9.1 x 10^{-7} -1.0 x 10^{-2} M response times ~ 8-10 sec and pH range 5.8-7.6. The proposed sensors show a reasonable discrimination ability towards Pb(II) in comparison to some alkali, alkaline earth, transition heavy metal ions. The modified electrodes were applied as an indicator electrode and successfully used to determine Pb(II) in drinking water samples giving satisfactory results.

CONTENTS

LIST OF TABLES

LIST OF FIGURES

LIST OF SCHEME

LIST OF ABBREVIATIONS

ISE	Ion-selective electrode**.**
PVC	Poly Vinyl Chloride
CWE	Coated wire electrode
CMCPE	Chemically modified carbon paste electrode**.**
SCE	Saturated calomel electrode
2-NPOE	2-nitrophenyl octyl ether
DBP	Dibutyl phthalate
DOP	Dioctyl phthalate
DOS	Dioctyl sebacate
DBBPh	Dibutyl butyl phosphonate
TEPh	Tris(2-ethylhexyl) phosphate
TBPh	Tributyl phosphate
BA	Benzyl acetate
TCP	Tricresyl phosphate.
SSM	Separate solution method
MPM	Matched potential method
FIM	Fixed Interference method

FPM	Fixed Primary Method
IUPAC	International Union of Pure And Applied Chemistry
ATBH	2-acetyl thiophenebenzoylhydrazone,
AFBH	2-acetylfuranbenzoylhydrazone
CTBH	2-carboxaldehydethiophenebenzoylhydrazone
CFBH	2-carboxaldehydefuranbenzoylhydrazone
emf	Electromotive force
UV-Vis	Ultravilot -visible region
DMF	Dimethylformamide
DMSO	Dimethylsulfoxide
EDTA	Ethylenediaminetetraacetic acid
$\mathbf{P}_{TLC}$	lipophilicity
εr	dielectric constants

AIM OF THE PRESENT WORK

Aim of the present work

1) Preparation of lead(II) complexes with the tridentate: SNO- and ONO- ligands, these scheme is shown in below.

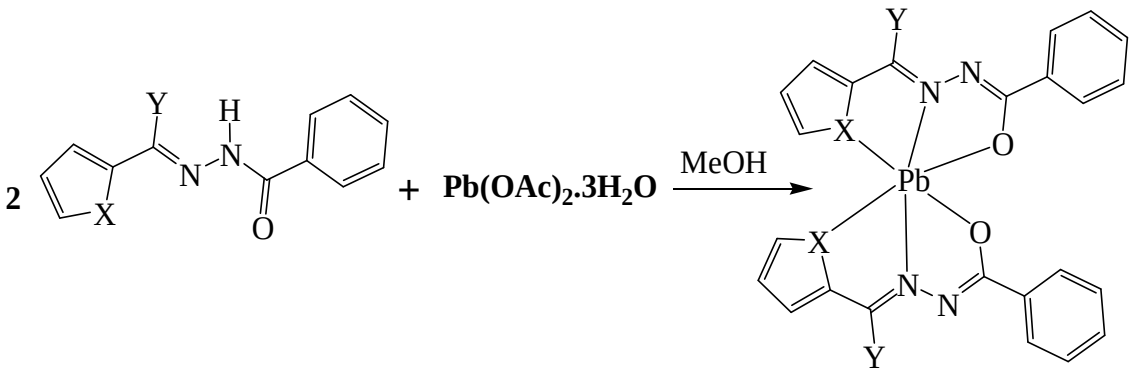

Scheme. preparation of lead (II) complexes.

X = S, O

Y = H, CH_3

2) Characterization of the product complexes by elemental analysis and spectral (IR, UV–vis and NMR) studies.

3) Use of these complexes as ionophores in preparation of chemically modified carbon paste electrode as lead(II) sensors.

4) Characterization of these electrodes by defining their properties such as detection limit, concentration range, response time, reproducibility, effect of pH, selectivity and effect of temperature**.**

5) Application of these electrodes for measuring Pb(II) in drinking water samples by using three methods namely potentiometric titration, standard addition method and calibration curve.

CHAPTER 1

INTRODUCTION

1.1 Coordination Compounds:

Coordination compounds are known as coordination complexes, complex compounds, or simply complexes. The essential feature of coordination compounds is that coordinate bonds form between electron pair donors, known as the ligands, and electron pair acceptors, the metal atoms or ions. The number of electron pairs donated to the metal is known as its coordination number. Although many complexes exist in which the coordination numbers are 3, 5, 7, or 8, the majority of complexes exhibit coordination numbers of 4, or 6. In order for a pair of electrons to be donated from a ligand to a metal ion, there must be an *empty* orbital on the metal ion to accept the pair of electrons. This situation is quite different from that where covalent bonds are being formed because in that case one electron in a bonding pair comes from each of the atoms held by the bond [1].

1.1.1 Geometry

In coordination chemistry, a complex is first described by its coordination number, the number of groups (ligands) attached to the metal (more specifically, the number of σ-type bonds between ligands and the central atom). Coordination numbers are normally between two and nine, but large numbers of ligands are common for the lanthanides and actinides. The number of bonds depends on the size, charge, and electron configuration of the metal ion and the ligands. Metal ions may have more than one coordination number. Typically the chemistry of complexes is dominated by interactions between s and p atomic orbitals of the ligands and the d orbitals of the metal ions [1]. The s, p, and d orbitals of the metal can accommodate 18 electrons. The maximum coordination number for a certain metal is thus related to the electronic configuration of the metal ion (more specifically, the number of empty orbitals) and to the ratio of the size of the ligands and the metal ion. Large metals and small ligands lead to high coordination numbers, e.g. $[Mo(CN)_8]^{4-}$. Small metals with large ligands lead to

low coordination numbers, e.g. $Pt[P(CMe_3)_3]_2$. Due to their large size, lanthanides and actinides tend to have high coordination numbers. The geometry of a complex depends basically on the coordination number. These structures are shown in Figure 1.1.

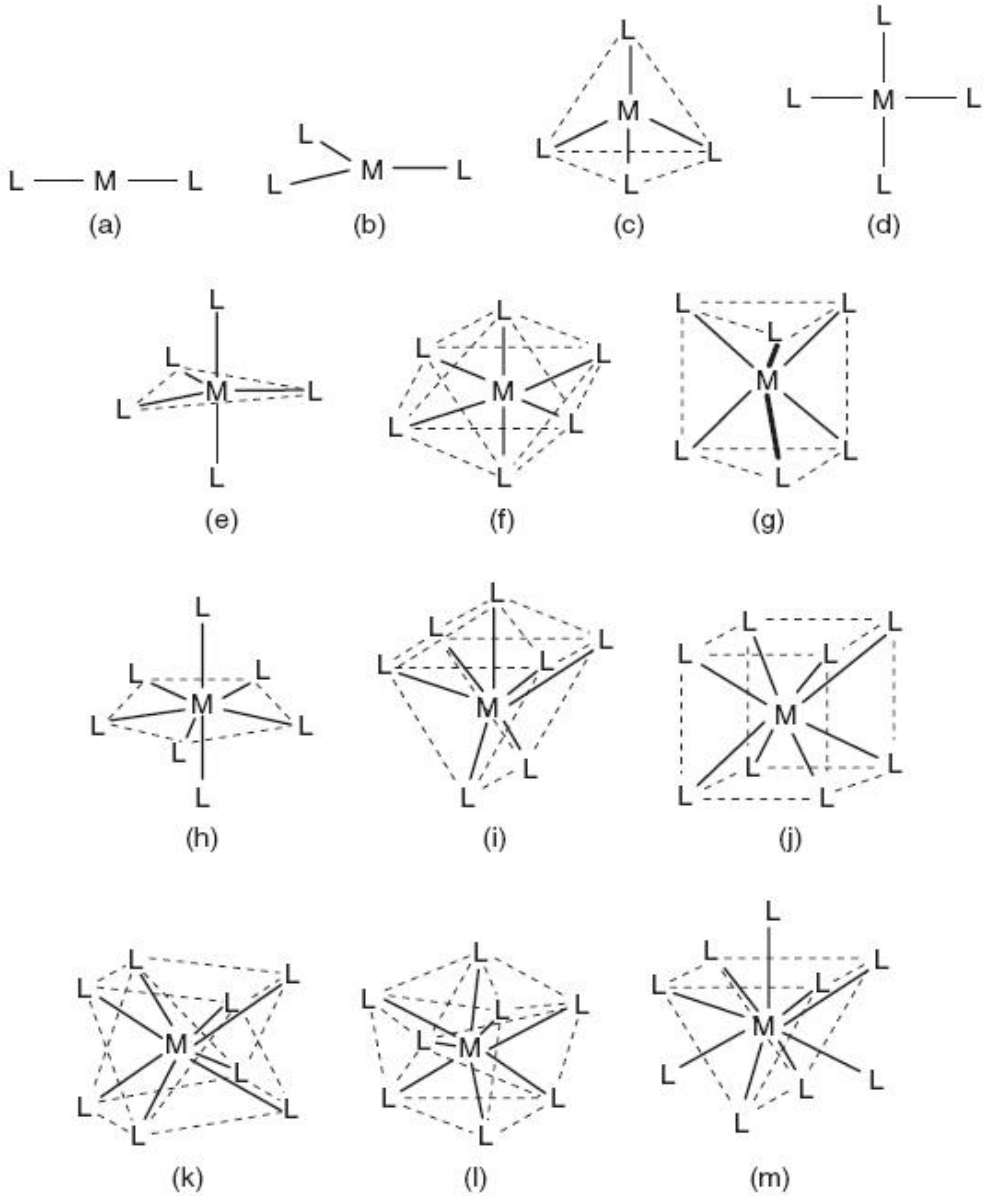

Figure 1.1 Some of the most common structures for coordination compounds: (a) linear; (b) trigonal planar; (c) tetrahedron; (d) square plane; (e) trigonal pyramid; (f) octahedron; (g) trigonal prism; (h) pentagonal bipyramid; (i) single-capped trigonal prism; (j) cubic; (k) Archimedes (square) antiprism; (l) dodecahedron; (m) triple-capped trigonal prism[1].

However the most observed geometries are listed below in Table (1.1), but there are many cases which deviate from the regular geometry, e.g. due to the use of ligands of different types.

Coordination number	Geometry
2	Linear
3	Trigonal planar, tri gonal pyramidal.
4	Tetrahedral or square planar
5	Trigonal bipyramidal or square pyramidal
6	Octahedral or trigonal prismatic
7	Pentagonal bipyramidal, Monocapped octahedron.
8	Dodecahedral; square antiprismatic; hexagonal bipyramidal
9	Tri-capped trigonal prismatic

Table1.1 Geometries for common coordination numbers.

1.1.2 Isomerism in coordination compounds

The arrangement of the ligands is fixed for a given complex, but in some cases it is changeable by a reaction that forms another stable isomer. There exist many kinds of isomerism in coordination complexes, just as in many other compounds.

1.1.2.1 Stereoisomerism

Stereoisomerism occurs with the same bonds in different orientations relative to one another. Stereoisomerism can be further classified in to :

1.1.2.1.a. Geometrical isomerism:

Cis-trans Isomerism and facial-meridional Isomerism:

Cis-trans isomerism occurs in octahedral and square planar complexes (but not tetrahedral). When two ligands are mutually adjacent they are said to be **cis**, and trans when opposite to each other. We have already observed that square complexes of the

type ML_2X_2 can exist as cis and trans isomers. Isomers of octahedral complexes ML_4X_2 can exist as cis and trans isomers[2]. When three identical ligands occupy one face of an octahedron, the isomer is said to be facial, or **fac**. In a fac isomer, any two identical ligands are adjacent or *cis* to each other. If these three ligands and the metal ion are in one plane, the isomer is said to be meridional, or **mer**. A mer isomer can be considered as a combination of a *trans* and a *cis*, since it contains both trans and cis pairs of identical ligands. Example ML_3X_3. These structures are shown in below [3].

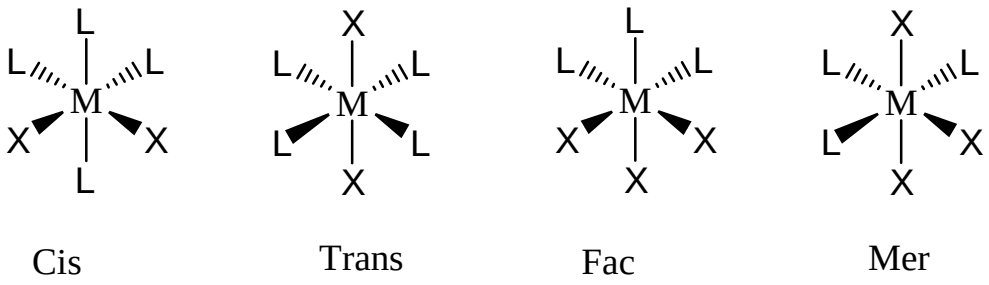

Isomers **Isomers**

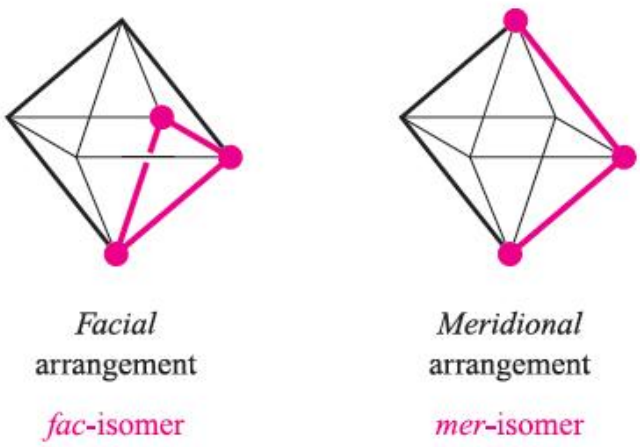

1.1.3 Electronic Properties of Metal Complexes

Many of the properties of metal complexes are dictated by their electronic structures. The electronic structure can be described by a relatively ionic model that ascribes formal charges to the metals and ligands. This approach is the essence of

crystal field theory (CFT). Crystal field theory, introduced by Hans Bethe in 1929, Crystal field theory is an electrostatic model which predicts that the d orbitals in a metal complex are not degenerate. The pattern of splitting of the d orbitals depends on the crystal field, this being determined by the arrangement and type of ligands [4], crystal field theory " provides a powerful yet simple method for understanding and correlating all of those properties that arise primarily from the presence of the partly filled shells " [2]. CFT gives a quantum mechanically based attempt at understanding complexes by considering all interactions in a complex as ionic and that the ligands can be approximated by negative point charges. More sophisticated models embrace covalency, and this approach is described by ligand field theory (LFT) and molecular orbital theory (MO). Ligand field theory, introduced in 1935 and built from molecular orbital theory, can handle a broader range of complexes and can explain complexes in which the interactions are covalent. The chemical applications of group theory can aid in the understanding of crystal or ligand field theory by allowing simple symmetry based solutions to the formal equations. Chemists tend to employ the simplest model required to predict the properties of interest; for this reason, CFT has been a favorite for the discussions when possible. MO and LF theories are more complicated, but provide a more realistic perspective. The electronic configuration of the complexes gives them some important properties [4].

1.1.3.1 Crystal Field Splitting

An important advance in understanding the spectra, structure, and magnetism of transition metal complexes is provided by crystal field model. The idea is to try to find out how the d orbitals of the transition metal are affected by the presence of ligands. The metal ion is considered to be placed first at the center of a hollow sphere of radius is equal to metal to ligand internuclear distance and that charge equal to the quantity

(ne-), that n is the number of ligands, is spread uniformly over the sphere. In this case the d orbitals are degenerate (have the same energy). As the ligand L approaches the metal from the directions of the polyhedron, the d orbitals that point toward the L groups are destabilized by concentrating the electron density of the ligands. Those that point away from L are stabilized variously from each other depending on the geometry. In octahedral complexes as the ligands L approach the metal ion along the x: y and z axes, the d orbitals will split as in figure 1.2-e. The d orbitals that are destabilized are the d_{x2-y2} and d_{z2}, those that are stabilized are d_{xy}, d_{yz}, and d_{xz}. The former pair of orbitals are often identified by their symmetry label, e_g, and the latter three have the label, t_{2g}. The magnitude of energy difference between the splitted d orbitals, is usually called the crystal field splitting and labeled Δ. For octahedral complexes the energy difference between t_{2g} and e_g is labeled Δ_o and depends on the nature of the ligand. The crystal field model works best when the symmetry is high, but with additional effort can be applied more generally for some distorted geometries or not high symmetric one. The idea is that orbitals closer to ligands will be destabilized more can be used to predict the splitting of d-orbitals in other geometries, in Figure 1.2 [2, 5].

1.1.4 Color

Metal complexes often have spectacular colors caused by electronic transitions by the absorption of light. Most transitions that are related to colored metal complexes are either **d-d transitions** or **charge transfer bands**. In a d-d transition, an electron in a d orbital on the metal is excited by a photon to another d orbital of higher energy. A charge transfer band entails promotion of an electron from a metal-based orbital into an empty ligand-based orbital (Metal-to-Ligand Charge Transfer or MLCT). The converse also occurs: excitation of an electron in a ligand-based orbital into an empty metal-

based orbital (Ligand to Metal Charge Transfer or LMCT). These phenomena can be observed with the aid of electronic spectroscopy, also known as UV-Vis [6].

For simple compounds with high symmetry, the d-d transitions can be assigned using Tanabe-Sugano diagrams. Increasingly, these assignments can be supported with computational chemistry [4].

1.1.5 Magnetic properties

The magnitude of the crystal field splitting also determines the magnetic properties of a complex, which depend on the number of unpaired electrons present. Ligands which give high crystal splitting are called high field, and that give low splitting are called low field. In octahedral complexes for d^1 through d^3 and d^8 through d^{10} ions, only one electron configuration is possible, so there is no difference in the net spin of electrons for strong and weak field cases. On the other hand, the d^4 through d^7 ions exhibit high and low spin states [7].

The actual arrangement of the electrons is determined by the amount of stability gained by having maximum parallel spins versus the investment in energy required to promote electrons to higher d orbitals, or in other words which is larger Δ_o or pairing energy (P). A useful rule that if $\Delta_o > P$ then low spin is expected, but if $\Delta_o < P$ high spin is the case. [2,8]. Δ_o is strongly dependent on the ligand, the metal and its oxidation state; effecting the electron configurations and the resulting spin [7].

1.1.6 Jahn-Teller Effect :

The Jahn–Teller theorem states that any non-linear molecular system in a degenerate electronic state will be unstable and will undergo distortion to form a system of lower symmetry and lower energy, thereby removing the degeneracy.

Jahn–Teller effects in tetrahedral complexes are illustrated by distortions in d^9 (e.g. $[CuCl_4]^{2-}$) and high-spin d^4 complexes. A particularly strong structural distortion is

observed in $[FeO_4]^{4-}$, Na_4FeO_4 contains discrete $[FeO_4]^{4-}$ ions. The high-spin d^4 configuration of Fe(IV) in $[FeO_4]^{4-}$ leads to a Jahn–Teller distortion, reducing the symmetry from Td to approximately D_2d [4]. These structures are shown in below.

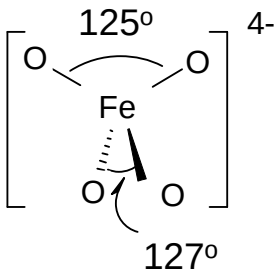

Average Fe-O = 181pm [4]

It is most pronounced when an odd number of electrons occupy the e_g orbitals; i.e. in d^9, low spin d^7, or high spin d^4, very common in six-coordinate copper(II) complexes. The d^9 electronic configuration of this ion gives three electrons in the two degenerate e_g orbitals, leading to unequal occupation, according to the theorem, such complex should distort so that the e_g orbitals are no longer degenerate. The distortion can take the form of either elongation or compression. Distortion from O_h to D_4h is the result, and its effect on d-splitting pattern is represented in Figure 1.2-f [7, 9].

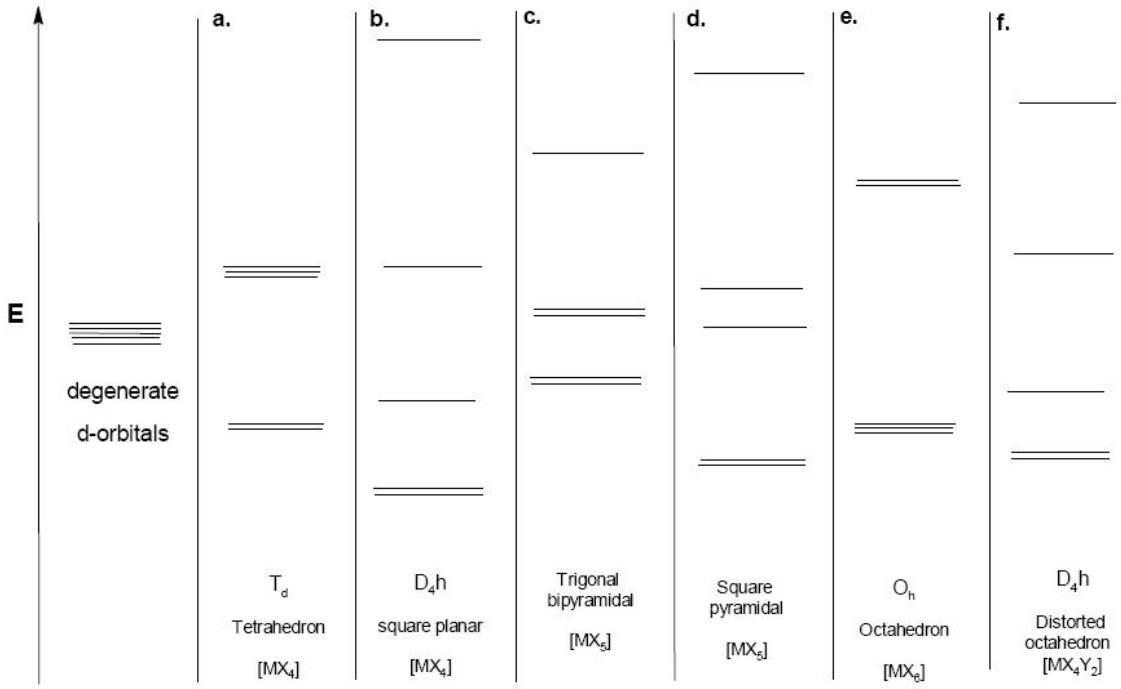

Figure 1.2: splitting of d-orbitals energy levels in ligand fields of common geometries for C.N. 4-6.

1.2 Ligands:

1.2.1 Strong Field and Weak Field Ligands

Ligands donate electrons to the central atom. Bonding is often described using the formalisms of molecular orbital theory. In general, electron pairs occupy the HOMO (Highest Occupied Molecular Orbital) of the ligands. Ligands and metal ions can be ordered in many ways; one ranking system focuses on ligand 'hardness'. Metal ions preferentially bind certain ligands. According to the molecular orbital theory, the HOMO of the ligand should have an energy that overlaps with the LUMO (Lowest Unoccupied Molecular Orbital) of the metal. Binding of the metal with the ligands results in a set of molecular orbitals, where the metal can be identified with a new HOMO and LUMO (the orbitals defining the properties and reactivity of the resulting complex). In an octahedral environment, the five otherwise degenerate d-orbitals split in sets of two and three orbitals [2].

three orbitals of low energy: d_{xy}, d_{xz} and d_{yz}

two orbitals of high energy: d_{z2} and d_{x2-y2}

The energy difference between these two sets of d-orbitals is called the splitting parameter, Δ_o. The magnitude of Δ_o is determined by the field-strength of the ligand: strong field ligands, by definition, increase Δ_o more than weak field ligands. Ligands can now be sorted according to the magnitude of Δ_o . This ordering of ligands is almost invariable for all metal ions and is called the spectrochemical series.

For tetrahedral complexes, the d-orbitals again split into two sets, but this time in reverse order, where

two orbitals of low energy: d_{z2} and d_{x2-y2} and

three orbitals of high energy: d_{xy}, d_{xz} and d_{yz}

The energy difference between these two sets of d-orbitals is now called Δ_t. The magnitude of Δ_t is smaller than for Δ_o, because in a tetrahedral complex only four ligands influence the d-orbitals, whereas in an octahedral complex the d-orbitals are influenced by six ligands. When the coordination number is neither octahedral nor tetrahedral, the splitting becomes correspondingly more complex. For the purposes of ranking ligands, however, the properties of the octahedral complexes and the resulting Δ_o have been of primary interest.

The arrangement of the d-orbitals on the central atom (as determined by the 'strength' of the ligand), has a strong effect on virtually all the properties of the resulting complexes. For example the energy differences of the d-orbitals has a strong effect on the optical absorption spectra of metal complexes. It turns out that valence electrons occupying orbitals with significant 3d-orbital character absorb in the 400-800 nm region of the spectrum (UV-visible range). The absorption of light (what we perceive as the color) by these electrons (that is, excitation of electrons from one orbital to another orbital under the influence of light) can be correlated to the ground state of the metal complex, which reflects the bonding properties of the ligands. The relative change in (relative) energy of the d-orbitals as a function of the field-strength of the ligands is described in Tanabe-Sugano diagrams [1].

In cases where the ligand has low energy LUMO, such orbitals also participate in the bonding. The metal-ligand bond can be further stabilized by a formal donation of electron density back to the ligand in a process known as *back-bonding.* In this case a filled, central-atom-based orbital donates density into the LUMO of the (coordinated) ligand. Carbon monoxide is the preeminent example a ligand that engages metals via back-donation [4]. Complementarily, ligands with low-energy filled orbitals of pi-symmetry can serve as pi-donor.

1.2.2 Spectrochemical series

It lists the common ligands in order of increasing Δ. This series can classify ligands to high field and low field ligands. *High field ligands* give rise to a large value of Δ; π-acceptor ligands are among this type where π-back bonding increases Δ. This type of ligands gives low spin complexes. *Low field ligands* give low Δ, that the spin pairing is lost and even the d^6 configuration can become paramagnetic. π-donor ligands follow this type, in which π-donor interaction decreases Δ. Some ligands can be listed to form a spectrochemical series, as below:

$I^- < Br^- < SCN^- < Cl^- < F^- < OH^- < OX^{-2} < \approx H_2O < NCS^- < NH_3 < en < bpy < phen < CN^- \approx CO.$

Weak field ligands ⟶ Strong field ligands

Some remarks should be considered when looking at the series: π-effects are not the only factor in determining Δ, that the effects on Δ by a given ligand are changed by other circumstances (different metal ion, different charge on the metal, other ligands present).[7,5].

1.2.3 Denticity

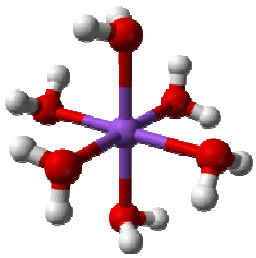

Atom with monodentate ligands

Denticity refers to the number of atoms in a single ligand that bind to a central atom in a coordination complex [10].

The word *denticity* is derived from *dentis*, the Latin word for tooth. The ligand is thought of as biting the metal at one or more linkage points. Denticity is distinguished

from hapticity, in which electrons of a bond or conjugated series of bonds are linked to the central metal without the metal-ligand bond being localized to a single ligand atom [11].

1.2.4 Types of Ligands According to Denticity

In many cases, only one atom in the ligand binds to the metal, so the denticity equals one, and the ligand is said to be **monodentate** (sometimes called **unidentate**). Ligands with more than one bonded atom are called **polydentate** or **multidentate.** Ligands can be classified according to the number of atoms in it that bind to the central atom:

1.2.4.1a. Unidentate ligands:

It is bound to a metal ion through a single donor atom, such as Cl, H_2O through oxygen atom, or acetate ion when it binds through only one of the oxygen atoms. In this case the ligand binds to the metal through a single point of attachment.

1.2.4.1b. Bidentate ligands:

Two donor atoms can be used to bind a metal ion, such as ethylene diamine $H_2NCH_2CH_2NH_2$, through the two nitrogen atoms. Bidentate ligands may be classified according to the number of atoms in it which separate the donor atoms, Figure1.3 below [3], and hence the size of the chelate ring formed with the metal ion.

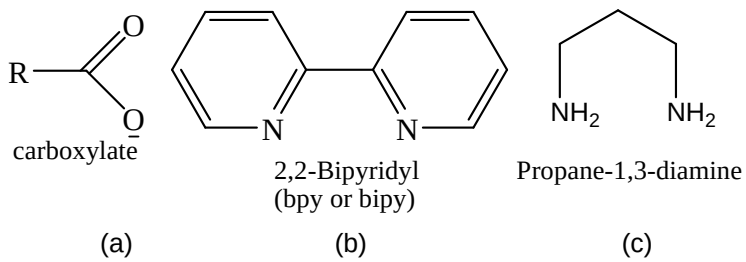

Figure (1.3) Examples of bidentate ligands (a) 1,1 ligands forming a four-membered ring (b) 1,2 bidentate a five-membered ring (c) 1,3 ligands a six-membered ring.

1.2.4.1c. Polydentate ligands:

Several donor atoms are present in a single ligand such as $N(CH_2CH_2NH_2)_3$ which binds through four nitrogen atoms, hence it is called tetradentate. The bidentate ligands mentioned above is part of this class of ligands; and was introduced separately because it can be thought as a building block for other polydentate ligands which can be imagined as a number of neighboring bidentate blocks, that can be in a planar or non-planar arrangement. When a bi or polydentate ligand uses two or more donor atoms to bind to a single metal, it is said to form a chelate complex. Examples of polydentate ligands are in Figure 1.4 [6].

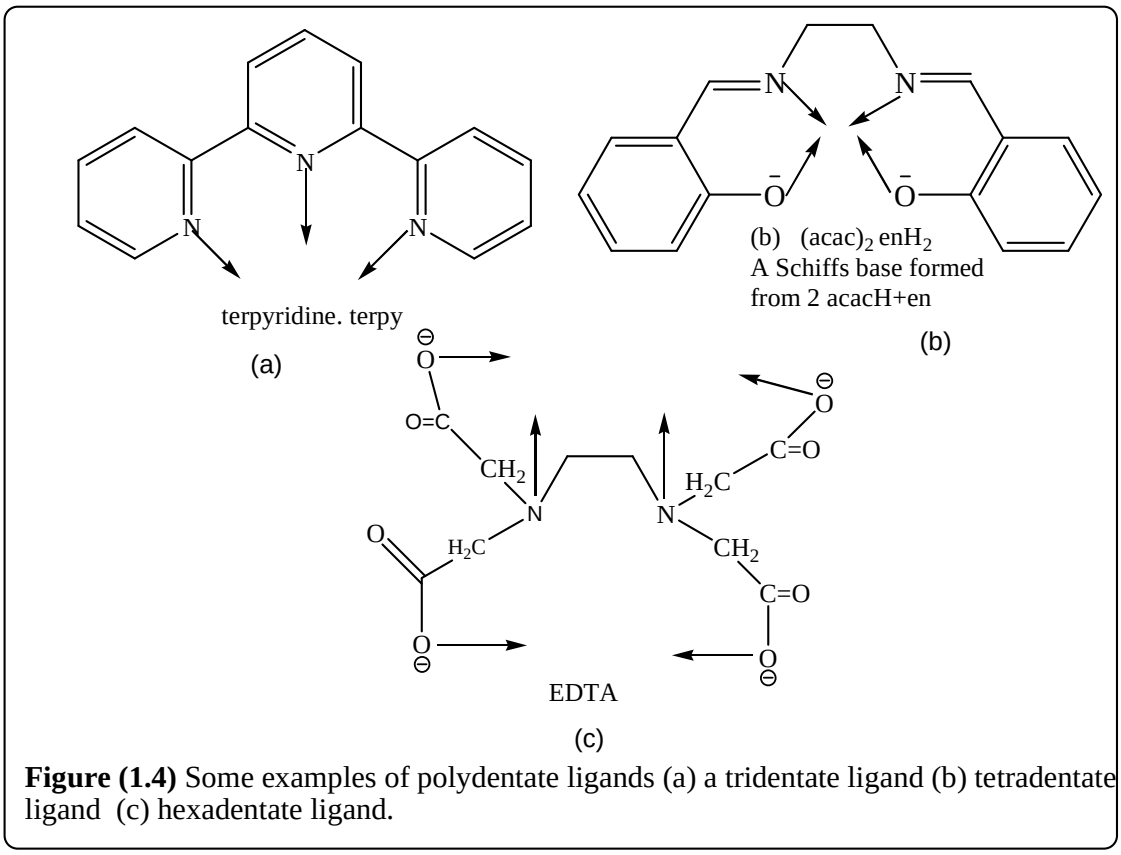

Figure (1.4) Some examples of polydentate ligands (a) a tridentate ligand (b) tetradentate ligand (c) hexadentate ligand.

1.2.4.1d. Macrocyclic proligands:

Ligands, They are cyclic compounds comprising a ring of at least nine atoms including at least three donor atoms oriented so as to bind to a metal ion. In a minimum

form a macrocyclic ligand would occupy three adjacent coordination sites on one side of a metal ion.

However, larger rings may have a central cavity large enough for the metal ion to fit into the plane of the macrocycle, such as porphyrin [11], these structures are shown in below [3].

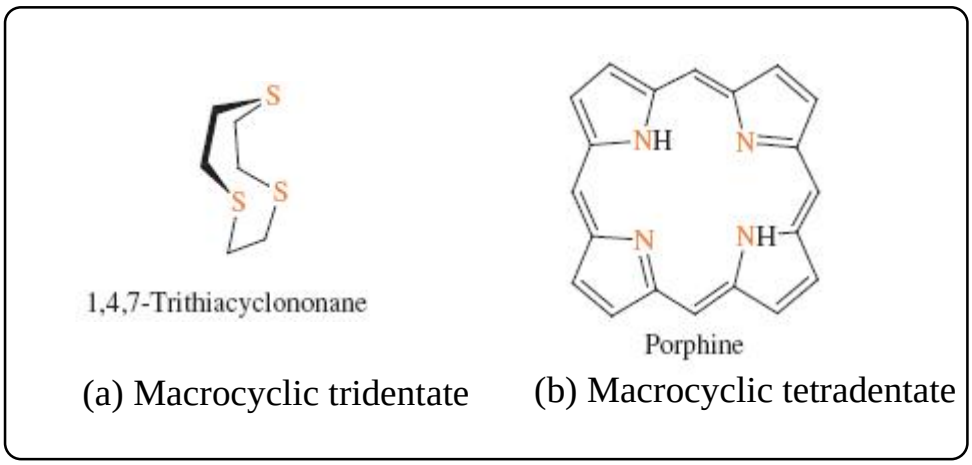

The term **proligand** may be used to refer to a species which may become a ligand through being bound to a metal ion but is not presently in a complex. In this text the symbols X, Y, Z will be used to represent ligands such as F, Cl, NH_3 or H_2O in which one donor atom is bound to the metal ion. The symbol L–L will be used to denote a ligand such as $H_2NCH_2CH_2NH_2$ which is bound to a metal ion through two donor atoms. The general symbol L will be used to represent a ligand of any type.

1.2.5. Donor and acceptor capabilities

Ligands can be sigma donor, pi-donor, or pi-acceptor.

a**. Sigma donors**: are σ-donors only, with no orbitals of appropriate symmetry for π-bonding, like ammonia NH_3. The ligand field split Δ, then depends on the relative energies of the metal ion and ligand orbitals and on the degree of overlap.

b**. Pi-donors**: have occupied p orbitals, they tend to donate these electrons to the metal along with the σ-bonding electrons, such as halogens.

c**. Pi-acceptors**: have vacant π* or d orbitals, there is the possibility of π-backbonding from the metal Figure 1.6. Examples are dithiocarbamate and CO, which have vacant π*, and PPh_3 which has vacant d orbital [7]. There are other types found in organometallic compounds, by using the highest occupied molecular orbital (HOMO) as the donor and the lowest unoccupied molecular orbital (LUMO) as the acceptor [5].

A π-donor ligand donates electrons to the metal centre in an interaction that involves a filled ligand orbital and an empty metal orbital; a π-acceptor ligand accepts electrons from the metal centre in an interaction that involves a filled metal orbital and an empty ligand orbital. π-Donor ligands include Cl^-, Br^- and $I^-$and the metal–ligand π-interaction involves transfer of electrons from filled ligand p orbitals to the metal centre (Figure 1.5a). Examples of π-acceptor ligands are CO, N_2, NO and alkenes. The metal–ligand π-bonds arise from the back donation of electrons from the metal centre to vacant antibonding orbitals on the ligand (for example, Figure 1.5b). π-Acceptor ligands can stabilize low oxidation state metal complexes [4].

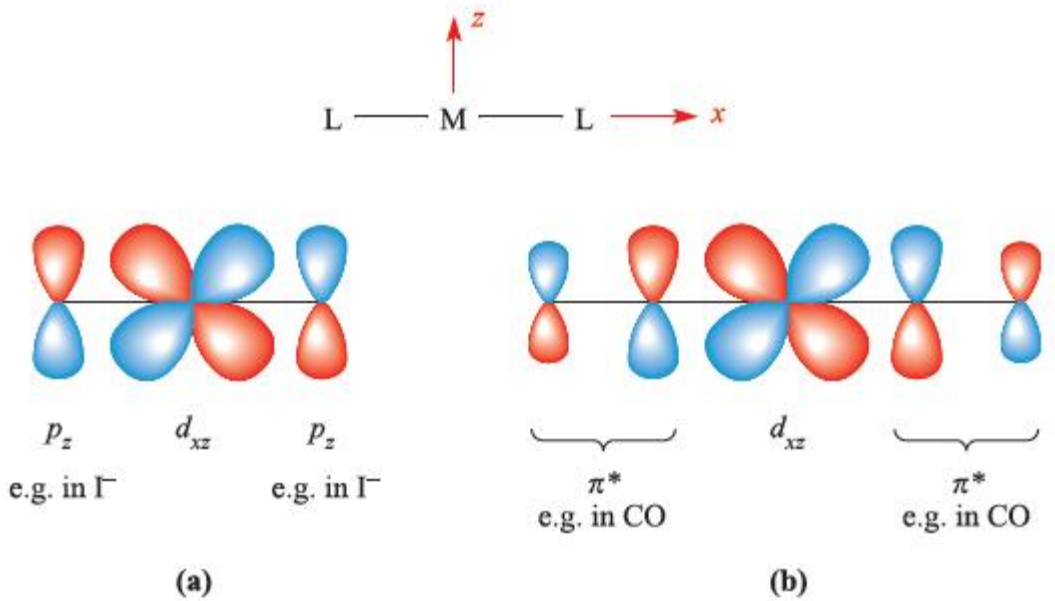

Figure (1.5) π-Bond formation in a linear L-M-L unit in which the metal and ligand donor atoms lie on the x axis: (a) between metal dxz and ligand pz orbitals as for L= I^-, an example of a π-donor ligand; and (b) between metal dxz and ligand π*-orbitals as for L = CO, an example of a π-acceptor ligand [4].

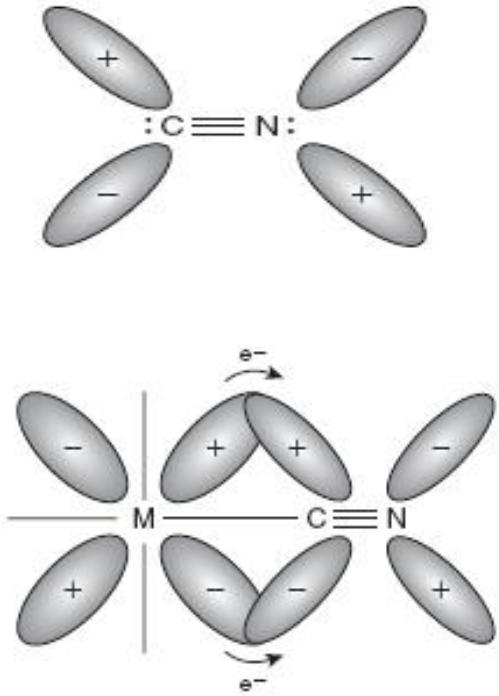

Figure (1.6). Back donation of electron density from metal \ orbitals to ligand π^* orbitals.[1]

1.2.6. The Nature of donor centers

Ligands and their properties vary as the donor centers or atoms vary.

1.2.6.1. Common elements function as donor atoms

Any of a variety of elements may function as donor atoms toward metal ions, but the most commonly encountered are probably nitrogen, phosphorous, oxygen, sulfur and the halides. In addition, a large number of compounds are known which contain carbon donor atoms (organometallic compounds) [11]. Some species are known by their ability to bind metal ions through certain atoms, such as heterocyclic compounds containing nitrogen, sulfur, or oxygen, and Schiff bases.

1.26.1.a. Schiff bases

A **Schiff base** (or **azomethine**), named after Hugo Schiff, is a functional group that contains a carbon-nitrogen double bond with the nitrogen atom connected to an aryl or alkyl group—but not hydrogen. Schiff bases are of the general formula $R^1R^2C=N-R^3$, where R^3 is an aryl or alkyl group that makes the Schiff base a stable imine. The structure are shown in below.

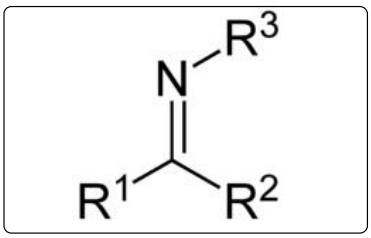

General chemical structure of a Schiff base

1.2.6.2. Single atom bonding motifs

1.2.6.2.a. Ambidentate ligands

Ligands that have more than one donor atom, but their geometrical arrangement does not allow them to bind to the same metal; i.e. they can not form a chelate ring. These ligands can be responsible for linkage isomerism, example SCN^- binding

through sulfur or nitrogen atom and DMSO binding through the lone pair on oxygen of S=O or through the π-bond it self, are examples [4].

1.3. Tridentate Ligands

A tridentate ligand has three donor atoms which is part of the polydentate ligands. Tridentate ligands are less common than bidentate and tetradentate ligands [2], but it has its own characteristics.

1.3.1. Rigidity of Tridentate Ligands

Tridentate ligands can be divided into rigid and flexible.

1.3.1.1. Rigid tridentate ligands

These ligands do not change the relative positions of their atoms and force the metal to fit itself with the ligand giving fixed structure. Rigid tridentate ligands can be planar or tripodal.

1.3.1.1.a. Planar tridentate ligands:

These ligands have the arrangement of their atoms in the same plane. Many of these ligands mainten π-conjugation that favors planarity markedly- example in figure 1.7a. Planar tridentate ligands in the octahedral geometry must form meridional complex.

1.3.1.1.b.Tripodal tridentate ligands:

have the general formula of $X(-Y)_3$, where X is a non donating atom or molecule and Y are the three donating centers. These ligands have structure like Figure 1.7b, they favor the facial coordination that is suitable for the fixed arrangement of their donating atoms [2, 11].

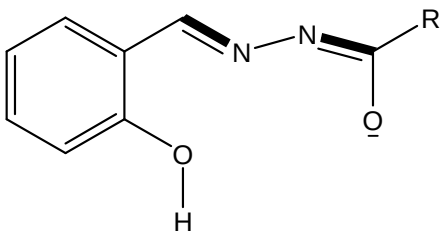

(a) (b)

Figure (1.7). Rigid tridentate ligands (a) planar tridentate ligand-acid hydrazide of salicaldehyde (b) tripodal tridentate ligands-1,3,5-Triaminocyclohexane.

1.3.1.2 Flexible Tridentate Ligands

This class can arrange its donor atoms and their relative positions such that more than one structural possibility can arise, for example diethylenetriamine, shown in Figure 1.8a, which is equally capable of meridional and facial coordination [11].

1.3.2 The Three Donor Centers

Tridentate ligands are different according to different donor atoms and their donor ability following their environment. Various systems can arise from these ligands.

1.3.2.1.a. Homoleptic tridentate ligands: Complexes in which a metal is bound to only one kind of donor groups, *e.g.* $[Co(NH_3)_6]^{3+}$, are known as **homoleptic** in Figure 1.8a.

1.3.2.1.b. Heteroleptic tridentate ligands: Complexes in which a metal is bound to more than one kind of donor group, *e.g.* $[Co(NH_3)_4Cl_2]^{+}$, are known as **heteroleptic**.in Figure 1.8b.

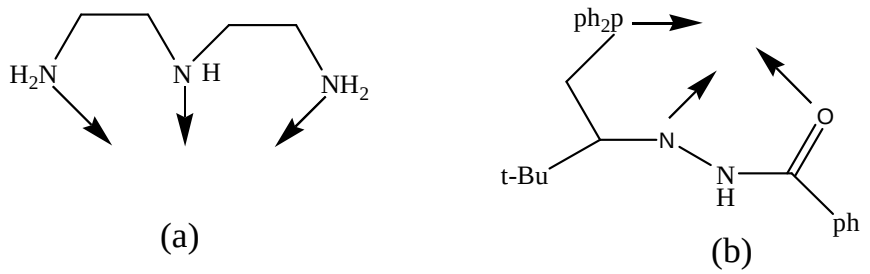

(a) (b)

Figure (1.8). More tridentate ligands (a) diethylenetriamine ligand (b) PNO donor ligand

1.4. Complexes of Tridentate Ligands

The tridentate ligands bind to metal ions through their three donor centers to form chelate complexes that have characteristic properties different from other kinds of complexes or chelates. As a result of this combination between the tridentate ligand and the metal ion every two adjacent donor atoms form a ring with the metal ion with a given size depending on the separation between these donor atoms.

1.4.1. Different Geometries

Tridentate ligands complexes have different geometries**,** for example the planar tridentate ligands favor the meridional octahedral or trigonal bipyramidal, that are suitable to their rigidity [2].

The most common geometries of complexes of tridentate with the first transition series are: octahedral, trigonal bipyramidal, square pyramidal and square planar.

1.4.2 Square Planar Complexes:

Are formed by small ligands and are d^8 electron configuration (Ni^{2+}, Pd^{2+}, Pt^{2+}, Au^{3+}), and Cu^{2+} (d^9), otherwise octahedral geometry preferred with cis/trans isomerism. The following Figures 1.9 show some examples: Figure 1.9a shows a square planar chelate [12], that needs one monodentate ligand besides the tridentate one to form four coordination number. Figure 1.9b describes an intermediate geometry between trigonal bipyramidal and square pyramidal of a five coordinated complex [13].

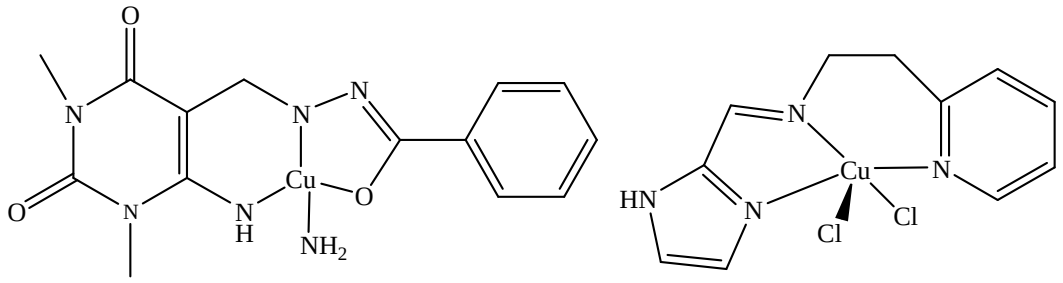

(a) (b)

Figure (1.9). Complexes of tridentate ligands (a) square planar complex of Cu^{+2} ion (b) five coordinate complex of tridentate ligand

1.4.3. Stability of complexes of tridentate ligands

Multidentate ligands are more stable than those with comparable monodentate ligands [14]. This trend continues as the number of donor atoms on the chelating ligands increases and increasing the number of chelating rings increase the stability of the complex.

1.4.3.1. Chelate Effect

As a general rule, a complex containing one (or more) five- or six-membered chalet rings is more stable (has a higher formation constant) than a complex that is as similar as possible but lacks some or all of the chelate rings [2].

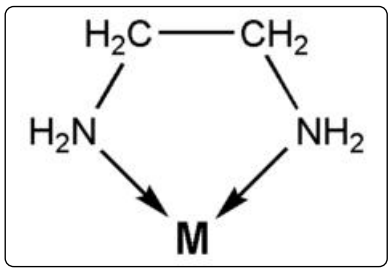

Ethylenediamine ligand, binding to a central metal ion with two bonds

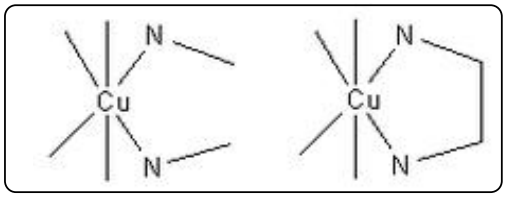

Cu^{2+} complexes with methylamine (left) and ethylenediamine (right)

1.4.3.2. Ring size

The most stable ring is the five membered ring. Two factors can illustrate this: A) an entropy effect useful in explaining the reason of reducing stability for larger rings, that when one end is bonded to the metal the longer the chain is the one that has the more vibrating unattached end, then it is the more ordered as coordinates to metal [15].

B) clarify the unfavorability for smaller rings, because the bond angle is significantly smaller than tetrahedral angle; that means it is a strain effect[14]. **Example of some SNO and ONO ligands .**

1.4.4. Octahedral bis (tridentate) systems

This class of complexes is stable according to the number of chelating rings it contains, for example if two planar tridentate ligands bound to metal ion, the complex will have four chelating rings. An example of this class is the 1:2 metal : tridentate ligand complex, in Figure 1.10 [16].

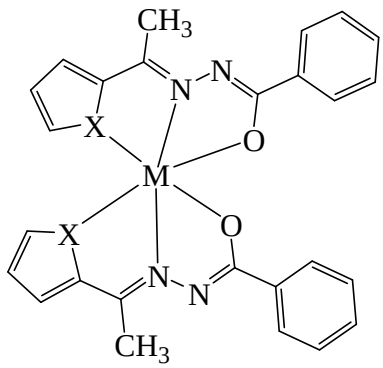

Figure (1.10) Complex of 1:2 metal to tridentate ligand ratio
" M = divalent metal ion (Co, Cu, Ni, Zn, or Pb).
" X = O, S, or N.

1.5. SNO and ONO Complexes

SNO and ONO complexes are those which contain tridentate ligands with sulfur, nitrogen, and oxygen donors atoms and oxygen, nitrogen and oxygen donors atoms. Nitrogen, sulfur and oxygen atoms are knowns electronegative donor atoms. To form stable chelates the ligand through its donor atoms should be basic. Tridentate ligands of SNO, ONO donors are generally Lewis base and donate electrons to the central metal (Lewis acid) in the complex.

Schiff base ligands with ONO donor atom have many structural, magnetic, spectroscopic and biological applications. For example, the study by M. Shebl on synthesis, spectral and magnetic studies of mono- and bi-nuclear metal complexes of a new bis(tridentate NO_2) Schiff base ligand derived from 4,6-diacetylresorcinol and ethanolamine [17].

Metal complexes of S-, N-, and O-chelating ligands have attracted the considerable attention because of their interesting physico-chemical properties, pronounced biological activities, and as models of metalloenzyme active sites For example, S. Patil, et. al. reported [18].

1.6. Ion-Selective Electrodes

Ion-selective electrodes (ISEs) belong to the oldest established chemical sensors. ISEs were applied in diverse fields of analysis such as clinical [19], pharmaceutical [20-23] and environmental chemistry [24]. They are cheap, selective, sensitive and applicable over a wide range of experimental conditions. Therefore, development of efficient ion-selective electrodes has always been desirable objectives for the scientists.

Ion selective electrodes (ISEs) are electrochemical sensors that allow potentiometric determination of the activity of certain ions in the presence of other ions in the sample solution. Potentiometric sensors are essentially passive electrochemical devices, in which changes in the electromotive force (emf) are monitored under zero current conditions [25]. The ISEs function is due to the phase-boundary processes. The phase boundary potential across the sample membrane interface is the result of the ion-selective charge separation at that interface. In accordance with this charge separation, only the membrane surface processes affect the potential [26].

1.6.1. Types of ion-selective electrodes

ISEs can be classified according to the type and composition of the sensor of the electrode into many categories, from which:

1- Glass-electrodes [27].

2- Solid state-electrodes [28,29].

3- Liquid membrane-electrodes [30,31].

4- Enzyme substrate electrodes [32,33].

5- Gas-Sensing electrodes [34].

6- Bacterial, tissue and immuno-electrodes [35,36].

7- Ion-selective field effect transistors [37,38].

Liquid membrane-electrodes have many applications [39] and will be our focus afterwards.

1.6.1.1. Liquid membrane electrodes

Liquid membrane electrodes are based on water-immiscible liquid substances impregnated in polymeric membrane. The membrane-active recognition can be achieved by a liquid ion exchanger [40] or by a neutral macrocyclic compound having molecular sized dimensions containing cavities to surround the target ions [41].

The membrane is interposed between a standard (internal) and the test (external) ion solution. The electrochemical cell, which comprises the membrane separating the internal and the external electrolytes, as well as the two (internal and external) reference electrodes (Figure 1.11). Assume that these solutions contain the same hydrophilic electrolyte, $M^+ A^-$, and M^+ is the counter cation of the ion exchanger in the membrane. A chemical driving force that depends on the activity of this ion in both phases causes M^+ to partition from the organic to the aqueous phase. Because M^+ carries a charge and no net current can flow, this driving force is counter balanced by the phase boundary potential. It builds up spontaneously as M^+ starts to cross the interface and leads to interfacial charge separation. The relationship between this interfacial potential, E_{pB}, and the ion activities on either side of the phase boundary is shown in equation (1-1) :

$$E_{PB} = \frac{RT}{zF} In \frac{k_m a_M(aq)}{a_M(org)} \quad \text{.....(1-1)}$$

in which $a_M(aq)$ and $a_M(org)$ are the activities of the ion in the aqueous and organic phases, respectively, with charge z, k_m is the single ion distribution coefficient describing the distribution of ion between the sample solution and the membrane phase,

R, T and F are the gas constant, the absolute temperature, and the Faraday constant, respectively [42].

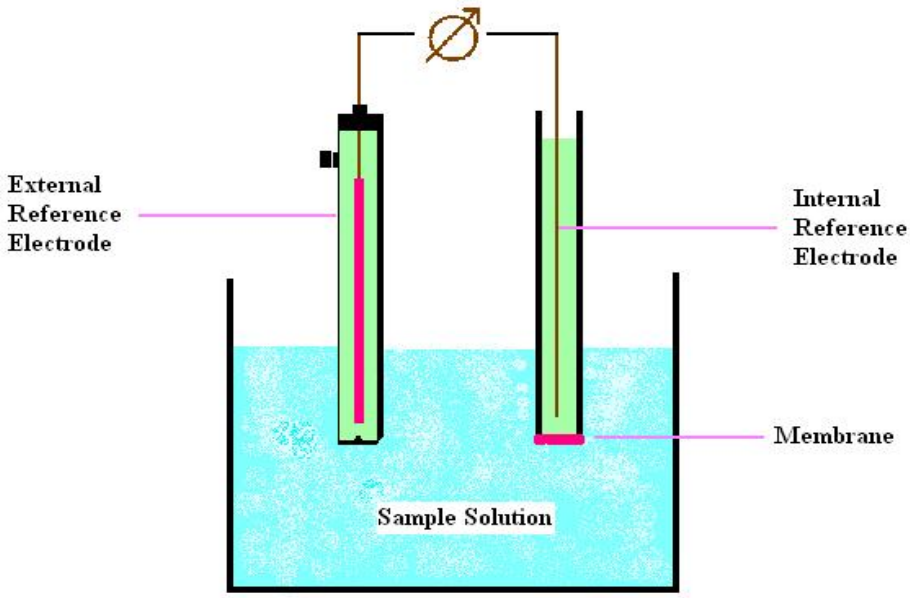

Figure (1.11) A classical ion-selective electrode ISE.

1.6.1.1.a. Conventional PVC membrane electrodes

The Poly vinyl chloride (PVC) principle for making conventional liquid membranes attracted much attention and was adopted by many workers for ISEs based on valinomycin and other neutral carrier sensors [43,44]. Indeed, the PVC matrix concept was the essential breakthrough that led to the almost universal clinical use of ISEs [45] for determining blood electrolytes [46,47] and for other applications [39].

1.6.1.1.b. Coated wire electrodes (CWEs)

Coated wire electrodes (CWEs) refer to a type of ISEs in which an electroactive species is incorporated in a thin polymeric support film coated directly on a metallic conductor. This moves to the total elimination of the internal filling solution and provides new advantage. Different materials can serve as central conductors. It was shown in an extensive study [48] that when the wire support did not react with the

membrane component, it had no substantial influence on the potentiometric response of the electrode. The substrate in the wire type electrodes is usually platinum wire, but silver, copper and graphite nodes have also been used. CWEs are prepared simply by dipping the central conductor into a solution containing dissolved polymer, plasticizer and electroactive substance and allowing the solvent to evaporate [49]. Some times CWEs exhibited better selectivity than conventional type electrodes with an internal solution. Simplicity of design, lower costs, mechanical flexibility of miniaturization and microfabrication widened the application for wire type electrode, especially in the fields of medicine and biotechnology.

1.6.1.1.c. Chemically modified carbon paste electrodes (CMCPEs) [50]

Over the past five decades, carbon paste, has become one of the most popular electrode materials used for the laboratory preparation of various electrodes, sensors [51]. Carbon paste electrodes are mixtures which are prepared from graphite powder and various water-immiscible organic liquids of nonelectrolytic character such as 2-nitrophenyl octyl ether (2-NPOE). This kind of carbon paste electrodes are classified as unmodified carbon electrodes [52-55]. Potentiometric carbon paste electrodes (CPEs) offer very attractive properties for the electrochemical investigation of inorganic and organic species over polymeric membrane and coated wire electrodes. These are ease of preparation and use, renewal of surface, chemical inertness, robustness, stability of response, no need of internal solution and suitability for a variety of sensing and detection application [56, 57].

From the viewpoint of equilibrium potentiometry, the composition of carbon paste enables the classification of CPEs as ion-selective liquid membrane type electrodes [58,59]. The electrodes themselves do not possess selectivity. However, by modifying

the electrode in a different compositions, degrees of selectivity may be introduced into the electrode itself and this can be done easily.

The modifying agent is usually one substance; but the paste can also be modified with two or even more components such as in the case of carbon paste-based biosensors that contain enzyme (or its carrier) together with an appropriate mediator [60] or CMCPEs with a mixture of two modifiers [61]. The amount of the modifier in the paste usually varies between 0.5-30% (w/w), depending on the character of modifying agent and its capability of forming enough active sites in modified paste (e.g., functional groups immobilized at the electrode surface) [62].

1.6.1.2. Membrane composition:

Any polymeric membrane ion selective sensor consists of some components. These components are : the polymeric matrix (polymer, carbon), the ionophore (membrane active recognition) and the membrane solvent (Plasticizer) [51]. The nature and the amount of each component have great effects on the nature and the characteristics of the sensor.

1.6.1.2.a. The Ionophore (membrane active recognition)

The ionophore, also named “ion carrier” is the most significant component of any polymeric membrane sensor for its selectivity and sensitivity which produces the response of the ISE in binding between the ionophore and the target ion. The different selectivities of an ISE toward the other ions, hence, may be considered to originate from the difference in the binding strength between any chosen ionophore, to be used in the sensor, and the various ions [51].

1.6.1.2.b. The Membrane solvent (plasticizer)

Plasticizers increase the plasticity or fluidity of the material, to which they are added. Solvent polymeric membranes, used in ion sensors, are usually based on a matrix containing about 40-60% (w/w) of a membrane solvent. In order to give a homogeneous organic phase, the membrane solvent must be physically compatible with the polymer, that is, display plasticizer properties. These properties influence the selectivity behavior. Some of the common plasticizers are: Benzyl acetate (BA), 2-nitrophenyl octyl ether (2-NPOE), dioctyl phthalate (DOP), dibutyl phthalate (DBP), tris(2-ethylhexyl) phosphate(TEPh), dioctyl sebacate (DOS), tributyl phosphate (TBPh) and dibutyl butyl phosphonate (DBBPh) [51].

1.6.2. Characterization of an ion-selective electrode

1.6.2.a. Measuring range

The linear range of the electrode is defined as that part of the calibration curve through which a linear regression would demonstrate that the data points do not deviate from linearity by more than 2 mV. For many electrodes, this range can extend from 1 M down to 10^{-6} or even 10^{-8} M [63].

1.6.2.b. Detection limit

The detection limit is the lowest concentration can be detected by the method. It can be calculated using the cross-section of the two extrapolated linear parts of the ion-selective calibration curve, according to the IUPAC recommendation. In practice, the values of the detection limit for most selective ISEs are in the range of 10^{-5} - 10^{-10} M [63].

1.6.2.c. Response time

It is well known that the dynamic response time of the modified electrode is one of the most important factors in its evaluation. The response time of the electrode is defined as the time between addition of the analyte to the sample solution and the time when a limiting potential has been reached [64].

1.6.2.d. Selectivity

Selectivity is the most important characteristic of these devices. It describes the ISE specificity toward the target ion in the presence of other ions, also called "interfering ions". There are a number of different methods for determination of the potentiometric selectivity coefficients (K_{XY}). The most important being: the Separate Solution Method (SSM), the mixed solution method (MSM), a. Fixed Interference method (FIM) b. Fixed Primary Method (FPM) and the matched potential method (MPM) [63].

1.6.2.e. Lifetime

The average lifetime for most of the reported ISEs is in the range of 2 to 10 weeks. After this time, the slope and the detection limit of the sensor will decrease and increase, respectively. Loss of the plasticizer, carrier or ionic site from the polymeric film, as a result of leaching into the sample, is the main reason for the limited lifetime of the carrier-based sensors [63].

1.6.2.f. Reproducibility

The closeness of agreement between independent results obtained with the same method on identical test martial but under different conditions (different operators, different apparatus, different laboratories, and/ or after different intervals of time) [65]. The measure of reproducibility is the standard deviation qualified with the term reproducibility as reproducibility standard deviation

1.6.3. Analytical methods that use electrochemical sensor :

1.6.3.a. Potentiometric determination:

In this method, the standard additions method was applied, in which a known incremental change is made through the addition of standard solution of the sample. This was achieved by adding known volumes of standard analyte ion solution to defined volume water containing different amounts of the investigated analyte in test solution with known amounts of analyte ion. The change in mV reading was recorded for each increment and used to calculate the concentration of the analyte in the sample solution using the following equation (1-2):

$$C_x = C_s\left(\frac{V_s}{V_x + V_s}\right)\left(10^{n(\Delta E/S)} - \frac{V_x}{V_s + V_x}\right)^{-1} \quad \ldots\ldots\ldots\ldots (1\text{-}2)$$

where C_x is the concentration to be determined, V_x is the volume of the original sample solution, V_s and C_s are the volume and concentration of the standard solution added to the sample to be analyzed, respectively, ΔE is the change in potential after addition of a certain volume of standard solution, and S is the slope of the calibration graph [66].

1.6.3.b. Potentiometric titrations:

In Potentiometric titration there is no need for calibration of the electrode before use. The electrochemical cell contains only the sample that has to be titrated. Step by step addition of the reagent is used and potential is recorded versus the volume of the reagent added. $C_R Ve = C_A V_A$ where C_R is the concentration of the reagent used for titration of the analyte, C_A is the concentration of the analyte, Ve is the volume at equivalence and VA is the volume of the sample. The rate of change of potentials for potentiometric titration is slow at the beginning of the titration, increases to a maximum as the equivalence point is passed. When the measured potential is plotted versus the

added volume of reagent, a double curve, like an elongated letter S, is obtained and the equivalence point is indicated at the steepest point of the curve, where the potential changes most rapidly [66].

1.6.3.c. Direct potentiometric methods or calibration curve method:

Direct potentiometry is the simplest and most widely used method of using ISEs. Simply measure the electrode response in an unknown solution and read the concentration directly from the calibration graph or from the meter display on a self-calibrating ion meter. A big advantage of this method is that it can be used to measure large batches of samples covering a wide range of concentrations very rapidly without having to change range, recalibrate or make any complicated calculations [66].

1.7. literature Survey

Lead was regarded by the ancients as the father of all metals and different civilizations used it extensively [67]. It is widespread, easy to extract, dense, highly malleable and stable to corrosion. However, with more evidence of lead toxicity and its adverse effects on human health, many of its applications were discontinued.

Nowadays, lead use is mostly restricted to the manufacture of batteries, metal alloys, glasses, ceramic and radiation shielding materials as well as some pigments and paint additives [67].

An increasing interest has emerged in synthesis and study of the properties of lead(II) compounds motivated partly by the necessity of understanding the Pb(II) binding preferences for the design of selective chelation therapy agents [68–72] and remediation of waters and soils [69, 73, 74].

Another topic is associated with the occurrence in Pb(II) compounds of a stereochemically active lone pair of electrons (LP, E) and its effect on the stereochemistry and properties of solid-state lead(II)-containing materials [75–78]. Despite the resurgence of interest in the structural chemistry and stereochemistry of Pb(II) complexes, there is a lack of systematic studies on this important class of compounds. The first review devoted to structural chemistry of Pb(II) compounds was published in 1976 by Harrison [79]. Along with the structures of Ge(II) and Sn(II) compounds, the review discusses the structures of some Pb(II) inorganic compounds. In a more complete form the crystal structures of Pb(II) compounds are presented in the review by the same author [80].

A detailed review of lead coordination and organometallic compounds is presented in a rather detailed work by Holloway and Melnik [81], in which more than 360 compounds were examined. About 20% are organometallic Pb(IV) compounds. The compounds are

divided into subgroups based on their nuclearity. The tables of crystallographic and structural data are presented in [81] for each coordination number (CN) of the Pb atom. The same authors have also reviewed the crystallographic and structural data of lead oxyacids and halide compounds [82] as well as heterometallic lead coordination and organometallic compounds [83].

Parr published a brief review of the coordination chemistry of Pb(II) in 1997 [84], followed by a more extensive review on Pb complexes the Comprehensive Coordination Chemistry II [85]. In a detailed review by Claudio et al. [69] devoted to the fundamental coordination chemistry, environmental chemistry, and biochemistry of Pb(II), one of the sections describes structural investigations on Pb(II) complexes. The stereochemistry of Pb(II) complexes with aminopolycarboxylate ligands and the role of LP for this class of compounds were reviewed [86]. In addition, the stereochemistry of Pb(II) complexes with oxygen donor ligands [87] and with sulfur and selenium donor ligands [88]. have been reviewed recently.

The electron configuration of Pb^{2+}, $[Xe]4f^{14}5d^{10}6s^2$, contains the $6s^2$ electron pair, which can be either stereochemically active or inactive in Pb(II) compounds. Based on the structural data presented in the Cambridge Structural Database (CSD) and ab initio molecular orbital optimizations, Shimoni-Livny et al. [89] investigated the role of the LP on the coordination geometry of the lead(II) ion. Based on the disposition of ligands around the metal ion, the authors [90] assigned the terminology described as "holodirected, in which the bonds to ligand atoms are directed throughout the surface of an encompassing globe" and "hemidirected, in which the bonds to ligand atoms are directed throughout only part of the globe, that is, there is an identifiable void (or gap) in the distribution of bonds to the ligands". The crystal structures of lead(II) compounds presented in the CSD adopt both *holodirected* and *hemidirected* coordination geometry

around the Pb atom. The geometry seems to strongly depend on the CN of Pb(II) and steric repulsion of the ligands.

Several methods for Pb^{2+} analysis have been developed in the past decade, including ones based on atomic absorption spectrometry (AAS) [91-111], atomic emission spectrometry (AES) [112-114], inductively coupled plasma mass spectrometry (ICP-MS) [115-134], anodic stripping voltammetry [135-157], and reversed-phase high-performance liquid chromatography coupled[158] with UV-vis or fluorescence detection [159-164]. With regard to sensitivity and accuracy, these methods are all efficient tools for Pb^{2+} detection, However, these methods comprise sample manipulation, extraction steps, derivatization

Reactions that are liable to various interferences as well as being not applicable to colored and turbid solutions these methods are expensive for they require large infrastructure backup and qualified personnel.

Thus, there is critical need for the development of selective inexpensive diagnostic tool for the determination of this analyte.

Analytical methods based on potentiometric detection with ion selective electrodes (ISEs) [165-181] can be considered a good alternative for their attractable characteristics. In the present study a modified carbon paste lead(II)-selective electrode have been constructed using the new lead(II) complex with 2-acetylthiophenebenzoylhydrazone (ATBH) as an excellent carrier. The influences of the carbon paste composition on the potential response of the Pb(II)-sensor was investigated.

CHAPTER 2

EXPEREMENTAL

2.1. Reagents and Materials

2-thiophenecarboxaldehyde, 2-furancarboxaldehyde and benzoylhydrazine were obtained from Merck. 2-acetylthiophene, 2-acetylfuran, graphite powder, 2-nitrophenyl octyl ether (2-NPOE), dioctyl phthalate (DOP), dibutyl phthalate (DBP), tris(2-ethylhexyl) phosphate (TEph), dioctyl sebacate (DOS), tributyl phosphate (TPh) and Tricresyl phosphate (TCP) were purchased from Aldrich.

The chlorides, nitrates, sulphates of the following cations, namely Na^{+}, K^{+}, NH_4^{+}, Li^{+}, Mg^{2+}, Cd^{2+}, Ba^{2+}, Ca^{2+}, Cu^{2+}, Zn^{2+}, Co^{2+}, Ce^{3+} and Al^{3+} were used as received, All solution were prepared in doubly distilled water.

2.2. Apparatus

The infra red spectra for the materials were recorded on a Perkin-Elmer FT-IR spectrometer using KBr disc in the range of 4000 to 400 cm^{-1}. Melting points were recorded on a Gallenkamp apparatus and are uncorrected. Uv-vis spectra of methanolic solutions of the complexes were recorded on a SHIMADZU UV-Visible spectrophotometer (UV-1601). Conductivity measurements were made on a PHYWE conductivity meter. The metal content of the complexes was determined using a Perkin Elmer A Analyst-100. The complexes were decomposed and digested in conc. sulfuric and/ or nitric acid before determination of the metal ions in their aqueous solutions (by atomic absorption, spectrophotometric or titrimetric methods). Microanalysis of C, H, N and S was performed at the University of Berlin-Germany. 1H-NMR and 13C NMR spectra were recorded on a Bruker 250-MHz spectrometer and JNM-ECS400 in DMSO-d6. Chemical shifts are in ppm relative to internal Me4Si. Potentiometric and pH measurments were made with a pocket pH / m V meters, pH 315i (wissen schaftlich-

technische werkstatten GmbH (WTW)- Germany) under stirring conditions at room temperature (25.0 ± 1.0 ◦C).

The performance of the electrodes was investigated by measuring the emfs of Pb2+ solutions with a concentration range of 10-7– 10-2 M by serial dilution. Each solution was stirred and the potential reading was recorded when it became stable, and plotted as a logarithmic function of Pb2+ activities which are calculated according to the Debye-Hückel equation (2-1),

$$\log \gamma = -0.511\, Z^2 [\mu^{1/2}(1+1.5\, \mu^{1/2}) - 0.2\, \mu] \ldots\ldots\ldots\ldots \quad (2\text{-}1)$$

which is applicable to any ion, where μ is the ionic strength and Z the charge [182].

2.3. Synthesis of the Schiff base ligands

The ligands: 2-acetyl thiophenebenzoylhydrazone (ATBH), 2-acetylfuranbenzoylhydrazone (AFBH), 2-carboxaldehydethiophenebenzoylhydrazone (CTBH) and 2-carboxaldehydefuranbenzoylhydrazone (CFBH) containing an SNO- or ONO- donor system, were prepared as described in the literature [183, 184].

2.4. Preparation of Pb(II) complexes

To a well-stirred suspension of the ligand (1.0 mmol) in methanol (25 mL) was added $Pb(OAc)_2.3H_2O$ (0.5 mmol, 0.19 g) solid. The resulting solution was stirred for 24 hours at room temperature during which a solid complex appeared. The solid was collected by filtration, washed with cold methanol, diethyl ether, and dried. The physical and chemical characterization of lead(II) complexes with the above mentioned ligands were made, collected and shown in schemes (2.1, 2.2, 2.3, 2.4) are shown in below.

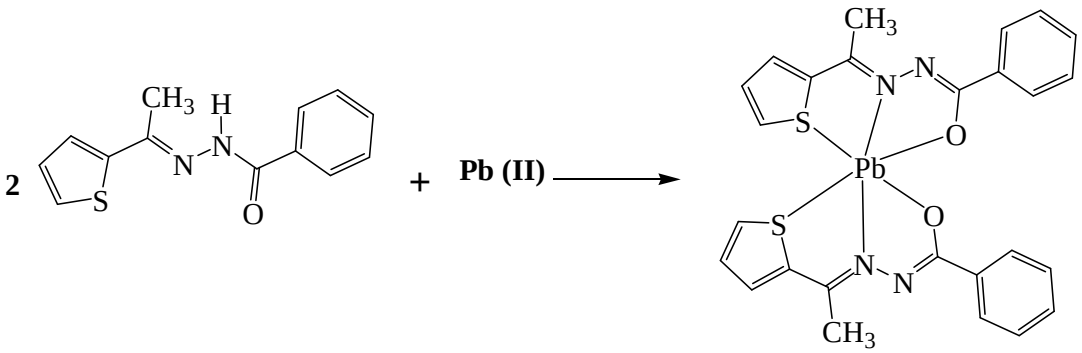

Scheme 2.1. structure of the schiff bases and thier lead (II) complexes.

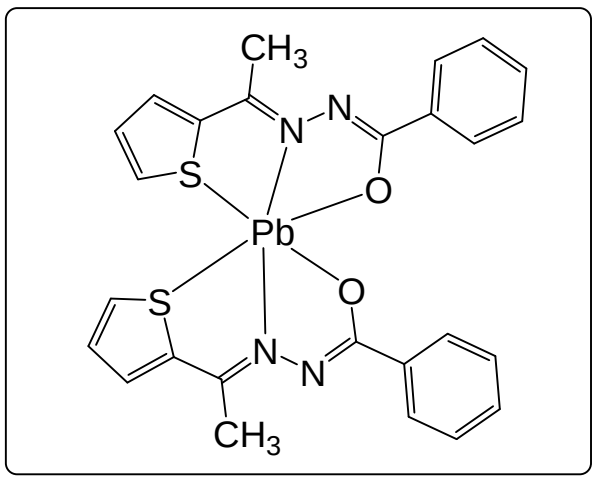

Pb(ATBH)$_2$

Pb(ATBH)$_2$ (L_1): yellow solid. Yield: 0.235 g (68 %). mp 255-7°C. Anal. Calcd. for $C_{26}H_{22}N_4O_2S_2Pb$: C, 45.01; H, 3.20; N,8.08, S: 9.24. Pb, 29.86, Found: C, 44.75; H, 3.15; N, 8.05; S: 9.20; Pb, 29.51

Λ_M (Mho cm^2 mol^{-1}): 7.4, UV/vis. (nm, logε): 314 (3.76), 260(3.10), Significant infrared bands (cm^{-1}): 1573 (C=N), 1163 (C-O), 1065 (C=N-N=C). ^{1}H-NMR: 8.18, 7.91, 7.88, 7.73, 7.40, 7.19 and 7.18 (ArH), 2.82 (C(CH$_3$)=N).

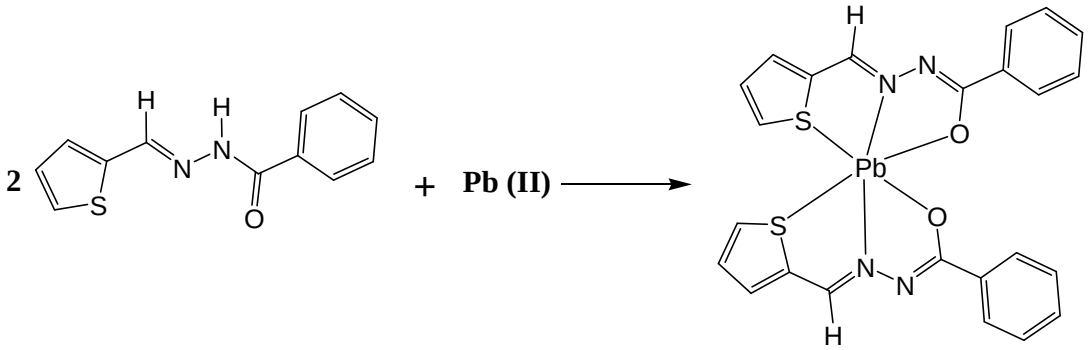

Scheme 2.2. structure of the schiff bases and thier lead (II) complexes.

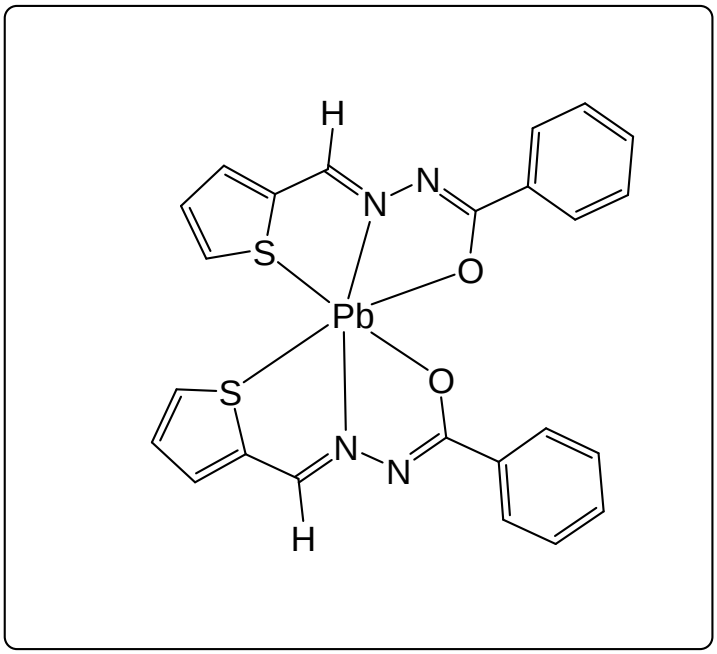

Pb(CTBH)$_2$

Pb(CTBH)$_2$ (L_2): yellow-tan solid. Yield: 0.218 g (65 %), mp 265-7 °C. Anal. Calcd. for $C_{24}H_{18}N_4O_2S_2Pb$: C, 43.30; H, 2.73; N,8.42, S: 9.63. Pb, 31.12, Found: C, 42.84; H, 2.70; N, 8.34; S, 9.59, Pb, 30.95, Λ_M (Mho cm^2 mol^{-1}): 22.1. UV/vis. (nm, logε): 322.5(3.101), 267(1.177), Significant infrared bands (cm^{-1}):. 1580 (C=N), 1169(C-O), 1051 (C=N-N=C), 469 (N→M), ^{1}H-NMR: 8.29, 7.86, 7.73 and 7.13 (ArH), 7.47 (HC=N).

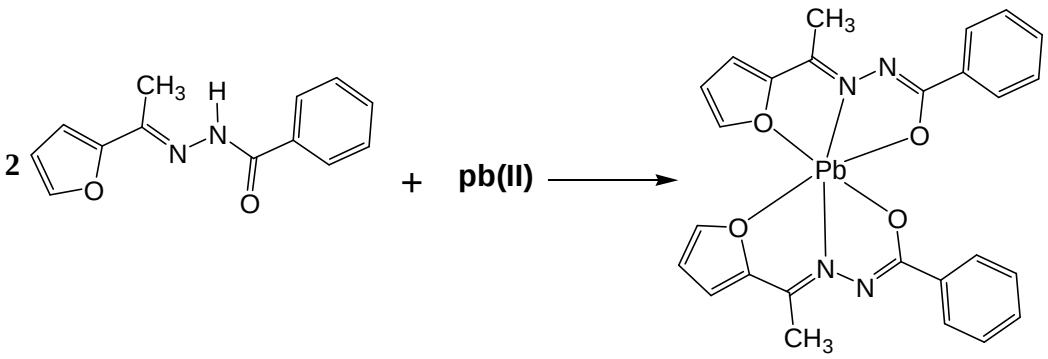

Scheme 2.3. structure of the schiff bases and thier lead (II) complexes.

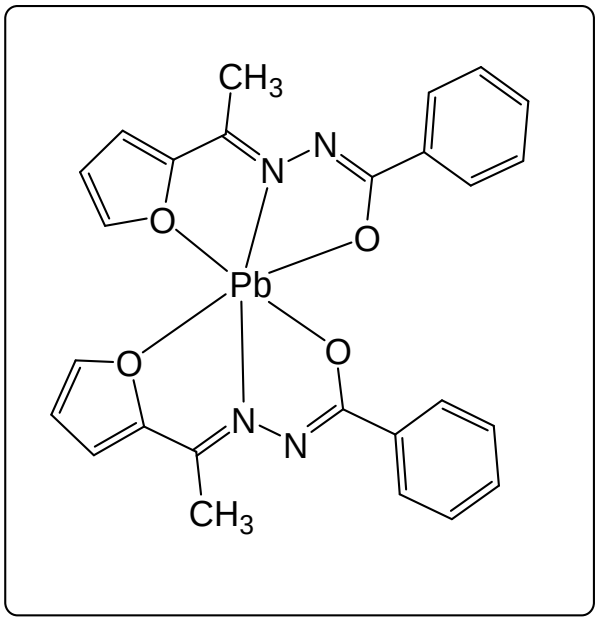

$Pb(AFBH)_2$

$Pb(AFBH)_2$ (L_3): pale tan solid. Yield: 0.210 g (63 %), mp 260-2 °C. Anal. Calcd. for $C_{26}H_{22}N_4O_4Pb$: C, 47.20; H, 3.35; N,8.47, Pb, 31.31, Found: C, 47.11; H, 3.32; N, 8.52; Pb, 30.94

Λ_M (Mho cm^2 mol^{-1}): 3.08. UV/vis. (nm, logε): 306(1.796), 252(2.658). Significant infrared bands (cm^{-1}): 1590 (C=N), 1502, 1359, 1164 (C-O), 1069 (C=N-N=C), 474 (N→M). ^{1}H-NMR: 8.53, 7.91, 7.75, 7.33, 7.01 and 6.72 (ArH) , 2.77 ($C(CH_3)$=N)

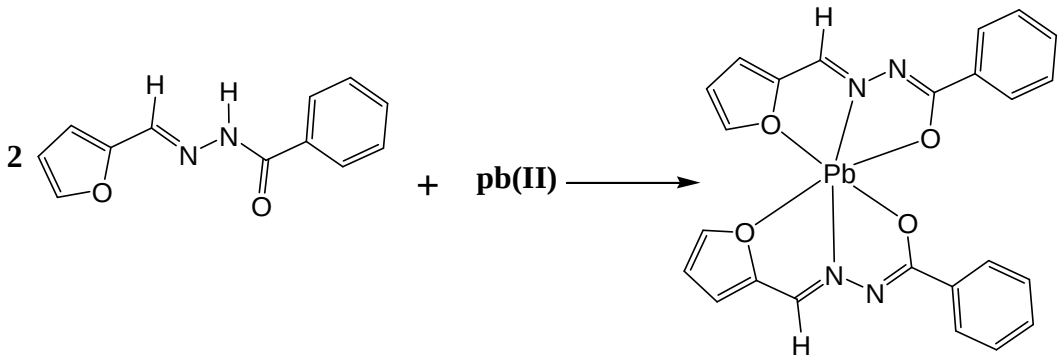

Scheme 2.4. structure of the schiff bases and thier lead (II) complexes.

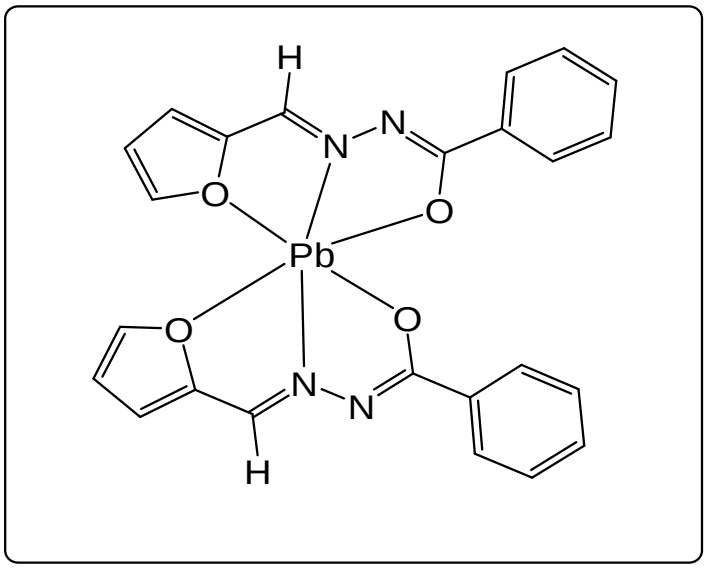

$Pb(CFBH)_2$

$Pb(CFBH)_2$ (L_4): pale tan solid. Yield: 0.198 g (62 %)., mp 280-2 °C. Anal. Calcd. for $C_{24}H_{18}N_4O_4Pb$: C, 45.49; H, 2.86; N,8.84. Pb, 32.70, Found: C, 45.71; H, 2.83; N, 8.92; Pb, 32.24. Λ_M (Mho cm^2 mol^{-1}): 10.48. UV/vis. (nm, logε): 310(2.383), 252(2.648), Significant infrared bands (cm^{-1}): 1613 (C=N), 1430(C-O), 1155(C=N-N=C), 441 (N→M). 1H-NMR: 7.92, 7.79, 7.32 and 6.71 (ArH), 7.15 (HC=N).

All the complexes have high melting points (>200°C). The results of elemental analysis are compiled in (Table 2.1). The electronic spectral data are collected in (Table 2.2) of all complexes.

Table (2.1) Yield, Color, Elemental analysis, Melting point, Molar conductance values of the compounds.

Compounds	% yield	color	Anal. Calcd.(found)%					m.p°C	Λ_M(Mho cm^2 mol^{-1})
			Pb	C	H	N	S		
$Pb(ATBH)_2$	68	Yellow solid	29.86 (29.51)	45.01 (44.75)	3..20 (3.15)	8.08 (8.05)	9.24 (9.20)	255-7	7.4
$Pb(CTBH)_2$	65	Yellow-tan solid	31.12 (30.95)	43.30 (42.84)	2.73 (2.70)	8.42 (8.34)	9.63 (9.59)	265-7	22.1
$Pb(AFBH)_2$	63	Pale-tan solid	31.31 (30.94)	47.20 (47.11)	3.35 (3.32)	8.47 (8.52)		260-2	3.08
$Pb(CFBH)_2$	62	Pale-tan solid	32.70 (32.24)	45.49 (45.71)	2.86 (2.83)	8.84 (8.92)		280-2	10.48

Table (2.2) UV spectral data of the compound.

Compounds	Electronic spectral data UV/vis. (nm, logε)
$Pb(ATBH)_2$	314(3.76), 260(3.10)
$Pb(CTBH)_2$	322.5(3.101), 267(1.177)
$Pb(AFBH)_2$	306(1.796), 252(2.658)
$Pb(CFBH)_2$	310(2.383), 252(2.648)

2.5. Preparation of Carbon Paste Electrodes

Unmodified carbon paste was prepared by intimate hand mixing of 154 mg of reagent grade graphite powder and 145 mg of different plasticizers in plastic Petri dishes using a glass rod as previously described [56]. The modified pastes were prepared in analogously, except that the graphite powder was mixed with the desired mass of the complex to get different compositions. Both unmodified and modified pastes were compactly packed into the end of a disposable polypropylene syringe (ca. 3 mm i.d. and 6 cm long) and electrical contact was achieved with a copper wire screw (Figure 2.1). The electrode surface was pressed against a filter paper to obtain intimate packing of the carbon paste and a smooth surface. A fresh surface of the paste was obtained by squeezing more out. The surplus paste was wiped out and the freshly exposed surface was polished on a paper until the surface showed shiny appearance and was used directly for potentiometric measurements without preconditioning requirements. The electrochemical system is represented as follows CMCPE/test solution//SCE.

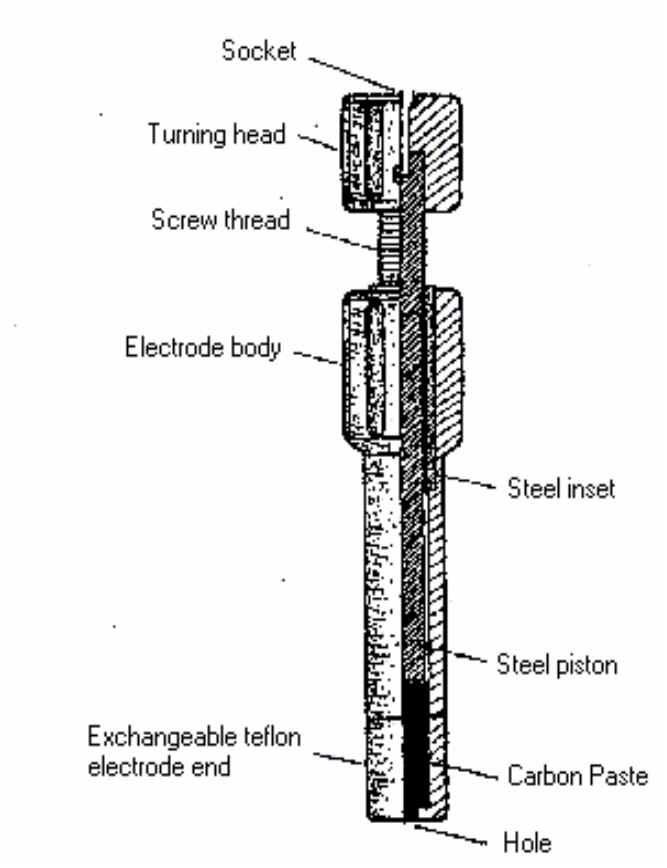

Figure 2.1 . A typical carbon paste electrode (cross section)

2.6. Construction of the Calibration Graphs

Suitable increments of standard lead ion solutions were added to 50 mL doubly distilled water so as to cover the concentration range 1.0 x 10^{-7}-1.0 x 10^{-2} M. The sensor and the reference electrodes were immersed in the solution and the emf value was recorded at 25.0±1.0 ˚C after each addition. The values were plotted versus the negative logarithmic value of the Pb^{2+} concentration.

2.7. Effect of pH on the Electrode Potential

The effect of pH of the test solution on the potential values of the electrode system in solutions of concentration 1.0x10^{-5} M Pb^{2+}, was studied. Aliquots of the lead ion solution (50 mL) were transferred to 100 ml titration cell and the tested ion-selective electrode in conjunction with the calomel reference electrode, and a combined glass electrode were immersed in the same solution. The pH of the solution was varied over the range 2.0-10.5 by addition of very small volumes of 0.1-1.0 M of HCl and NaOH solution. The mV-reading were plotted against the pH-values for the different concentration.

2.8. Effect of Temperature on the Electrode Potential

To study the thermal stability of the electrode, calibration graphs were constructed at different test solution-temperatures covering the range 20-50°C. The slope, usable concentration range and response time of the electrodes were determined at each temperature.

2.9. Effect of Interfering Ions on ISEs

The separate solution method (SSM) was applied. which requires two potential measurements. The first is the potential measured in a solution containing a known

amount of the ion for which the electrode is selective and the second is the potential measured in a solution containing the interfering ion. These potential values were used to calculate the selectivity coefficient value using the following equation(2-2):

$$\log K^{pot}_{Pb+2/J^{z+}} = \frac{E_2 - E_1}{S} + \log [\ Pb+2\ ] - \log [J^{z+}]^{1/z} \quad \ldots\ldots\ldots (2\text{-}2)$$

where $\log K^{pot}_{Pb+2/J^{z+}}$ is the selectivity coefficient value E_1 and E_2 are the electrode potentials of 10^{-3} M solution of each of the investigated Pb^{+2} and interferent cation, J^{z+}, respectively and S is the slope of the calibration graph.

2.10. Sample Analysis:-

2.10.1. Potentiometric determination of Pb^{+2} solution:-

2.10.1.a. Standard additions method

Standard addition methods in which small increments (10-100 µl) of (0.1 M) Pb^{2+} solution were added to 50 mL aliquot-samples of various concentrations ($5.0x10^{-6}$ M to $5.0x10^{-5}$M) Pb^{2+} was applied.

The change in mV reading was recorded for each increment and used to calculate the concentration of the Pb^{2+} in sample solution using the following equation(2-3):[66].

$$C_x = C_s\left(\frac{V_s}{V_x + V_s}\right)\left(10^{n(\Delta E/S)} - \frac{V_x}{V_s + V_x}\right)^{-1} \quad \ldots\ldots (2\text{-}3)$$

where C_x is the concentration to be determined, V_x is the volume of the original sample solution, V_s and C_s are the volume and concentration of the standard solution added to the sample to be analyzed, respectively, ΔE is the change in potential after addition of certain volume of standard solution, and S is the slope of the calibration graph.

2.10.1. b. Potentiometric titrations:

Different volumes of 1.0 x 10^{-3} M and 1.0 x 10^{-2} M equivalent to 1.035 -14.5 mg of the Pb^{2+}, were transferred to a 25 mL beaker, and titrated with a standard solution of EDTA using the prepared **lead**-electrode as indicator electrodes. The end points were determined from the S-shaped curves.

2.10.1. c. Calibration curve method

different amounts of Pb^{2+} were added to 50 mL of water comprising a concentration range from 5.9 x 10^{-7} M to 1.0 x 10^{-2} M and the measured potential was recorded using the present electrode. Data were plotted as potential versus logarithm of the Pb^{2+} activity and the resulting graph was used for subsequent determination of unknown Pb^{2+} concentration [185].

CHAPTER 3

RESULTS AND DISCUSSION

RESULTS AND DISCUSSION

The reaction of lead(II) acetate with the Schiff base ligands: 2-acetylthiophenebenzoylhydrazone (ATBH), 2-carboxythiophenebenzoylhydrazone (CTBH), 2-acetylfuranbenzoylhydrazone (AFBH) and 2-carboxyfuranbenzoylhydrazone (CFBH) in methanolic solutions gave monomeric lead(II) complexes, with the formula PbL_2 in which the ligands are tridentate. The formulations were in accordance with the results of elemental analysis and physicochemical measurements. The complexes are soluble in dimethyl formamide, and dimethyl sulfoxide, but are not soluble in common organic solvents. The molar conductance of the complexes at a concentration of ca. 1×10^{-3} M in DMSO have small values in the range 1.0- 22.1 μ Mho cm^2 mol^{-1}, indicating that the complexes are non-electrolytes.

3.1. Spectral Properties.

The IR spectrum of the ligands have several prominent bands appearing at about 3180 and 1670 cm^{-1} due to νN-H and νC=O stretching modes, respectively. Both these bands disappeared on complexation and a new νC-O band at 1237 cm^{-1} appeared. Comparison of the IR spectra of the Schiff bases with those of their lead(II) complexes, such as Figures 3.1 (a, b, c, d). complete IR data are presented in experimental part.

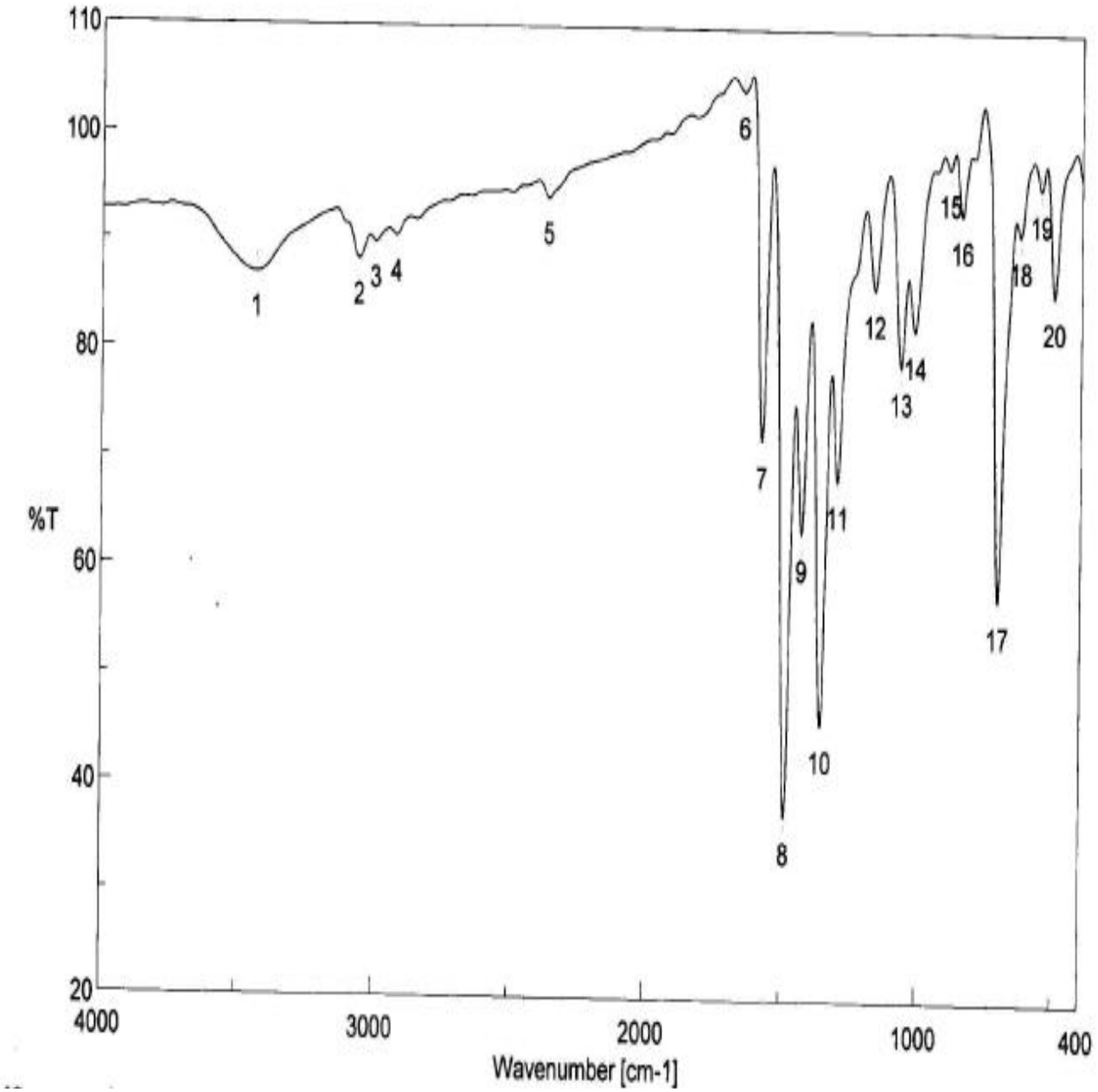

Figure 3.1(a) The infrared spectrum of the complex $Pb(ATBH)_2$

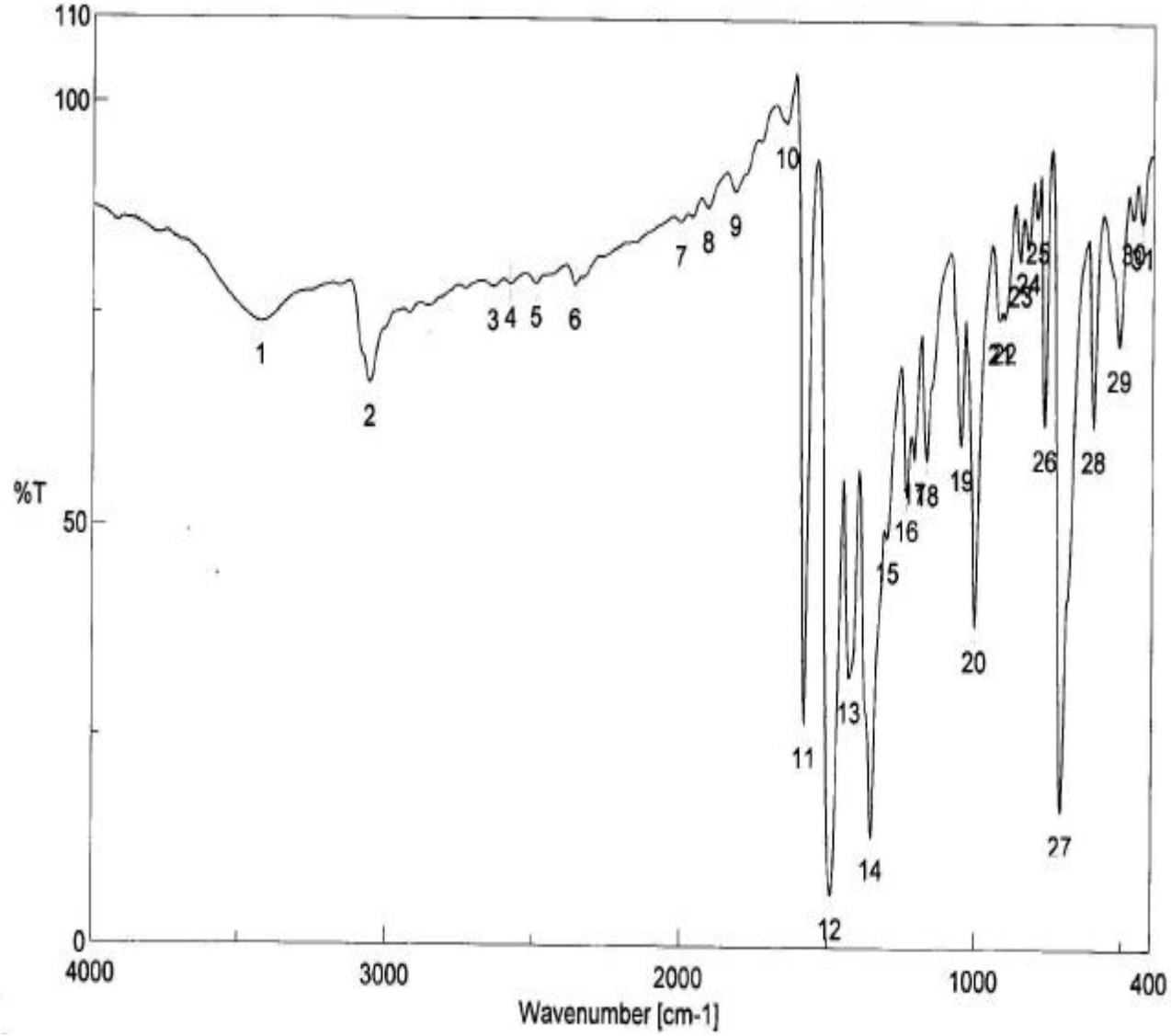

Figure 3.1(b) The infrared spectrum of the complex $Pb(CTBH)_2$

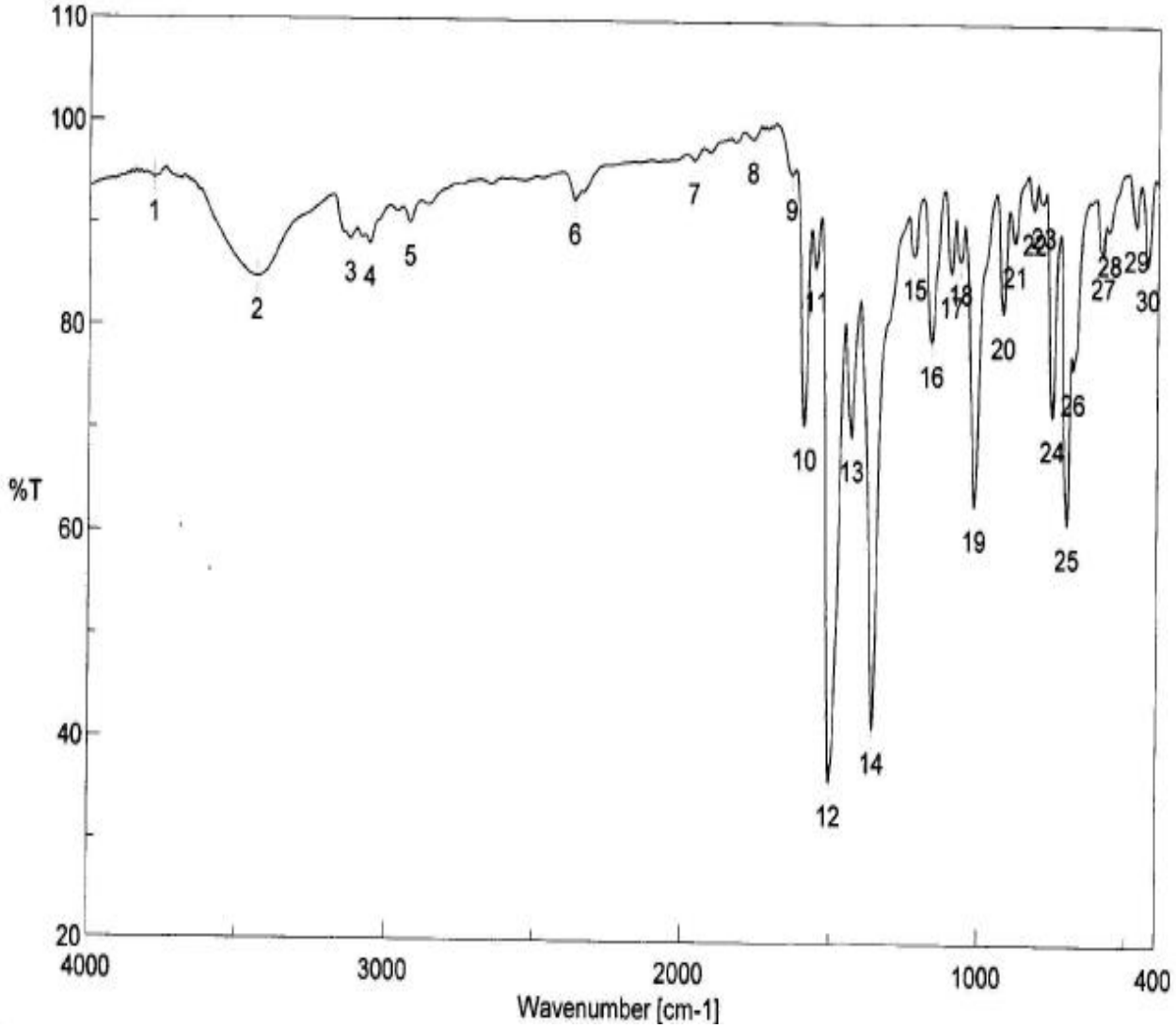

Figure 3.1(c) The infrared spectrum of the complex $Pb(AFBH)_2$

.

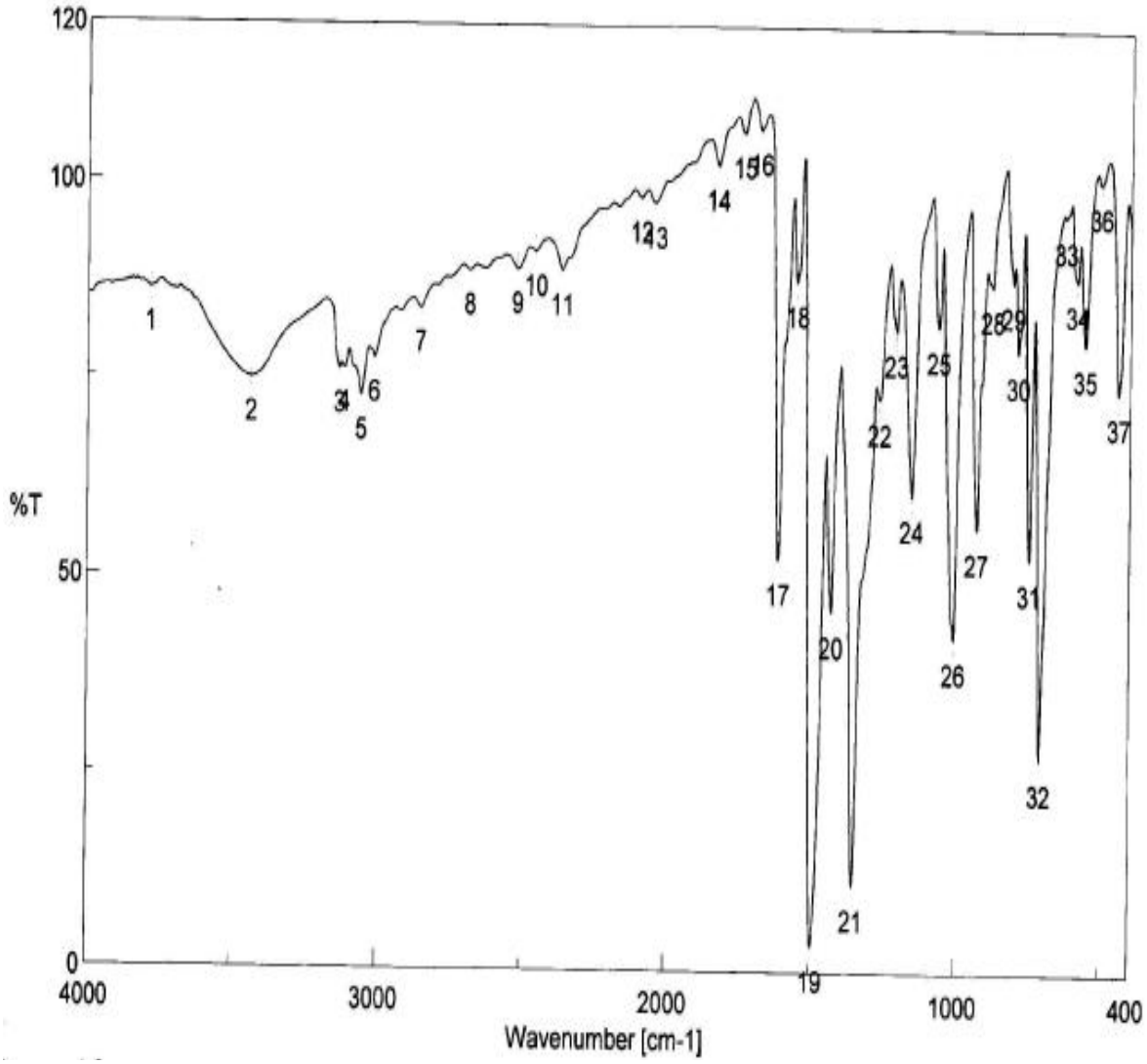

Figure 3.1(d) The infrared spectrum of the complex $Pb(CFBH)_2$

.

IR spectra indicates that the Schiff bases are coordinated to Pb(II) by three sites, that is the ligands are tridentate. That the band due to *ν*(C=O) is completely missing in the spectra of the complexes, suggests [186] (Patil et al., 1982) enolization of the Schiff base on complexation. This is supported by the fact that no band for *ν*(OH) is observed in the infrared spectra of the ligands and their lead(II) complexes. Instead, a band due to *ν*(C–O) at about 1237 cm^{-1} was observed for all the complexes, which supports the observation of their enolization during coordination. This fact suggests that the Schiff base remains in the keto form in the solid state, but in solution both the keto and enol forms remain in equilibrium [187].

Deprotonation occurs from the enol form on complexation. The amide-II band [ν(NH, CN] was split, displaced to higher frequency and reduced in intensity. A shift to higher frequency (5–10 cm^{-1}) of the ν(N–N) band at about 1020 cm^{-1} and its splitting [188] indicates coordination of the azomethine nitrogen. The *ν*(C-S-C) undergoes a negative shift in the complexes, indicating the coordination of the ring sulfur to the metal. The coordination through the azomethine nitrogen and sulfur is further supported by the occurrence on few bands at 460 and 360 cm^{-1} in the spectra of the thiophene complexes, which may be assigned to *ν*(N→M) and *ν*(S→M) vibrations respectively [189]. However, the IR spectrum of the complex (M-S) bands could not be observed because the spectra of the samples were studied in the range 4000-400 cm^{-1} which does not span the M-S stretching mode.

The ^{1}H-NMR spectra of the lead(II) complexes of these lignads Figure 3.2 have been recorded in DMSO-d_6. Comparison of the ^{1}H-NMR spectra of the free ligands and those of the complexes supports the conclusions derived from the IR spectra.

The ^{1}H-NMR of free ATBH showed the bands at 10.91, 7.43-8.64, and 2.48 ppm associated with the δ (N-H), δ (ArH), and δ ($C(CH_3)$=N) resonances, respectively. On complexation, the NH proton resonance at 10.91 ppm of the free ligand disappered, and the resonance for the aromatic and azomethine methyl proton are observed at 7.17- 8.18 and 2.82 ppm, respectively. This fact suggests

that the Schiff base acts as a monobasic tridentate ligand with acetylthiophene sulfur, azomethine nitrogen, and oxygen donor atoms in the enol form by tautomerism. In the Pb(II) complexes, the aromatic and heteroaromatic proton signals appeared downfield, due to increased conjugation on coordination [190].

The ^{1}H-NMR of $Pb(CTBH)_2$ is similar to that of $Pb(ATBH)_2$ except that the signal due to the methyl protons is missing and another band due to HC=N appears around 7.4 ppm. The signals due to the aromatic and the heteroaromatic protons appear at 7.11- 8.31 ppm. In addition, the ^{1}H-NMR of $Pb(AFBH)_2$ is similar to that of $Pb(ATBH)_2$ except that the band due to the methyl protons appear at 2.77 ppm and those due to the aromatic and the heteroaromatic protons appear at 6.72- 8.27 ppm. Again, the ^{1}H-NMR of $Pb(CFBH)_2$ is similar to that of $Pb(AFBH)_2$ except that the signal due to the methyl protons is missing and another band due to HC=N appears around 7.2 ppm. ^{13}C NMR spectra likewise, showed similar diagnostic features for the free ligands as well as their complexes. For example, the ^{13}C NMR spectrum of $(AFBH)_2Pb$ (Figure 3.3) contains a peak for every type of carbon in the complex: namely at 172.09 ppm for (O-C=N); at 150.02 ppm for (-C=N); at 149.52-112.38 ppm (eight signals) for the aromatic carbons (Ar-C) and at 15.04 ppm for ($-CH_3$). Similarly, the presence of the C=O signal at about 176 ppm in the spectra of the ligand and the absence of this signal in the spectra of the complexes and the appearance of a signal at a lower value supported the evidence that the ligands act in an enolized form.

The electronic spectra of the DMSO solutions of the free ligand, recorded in the region 250 – 800 nm exhibit bands in the range 250 – 280 and 300 – 340 nm assigned to the $\pi \rightarrow \pi^*$ and $n \rightarrow \pi^*$ transitions respectively of the azomethine group and are shifted to longer wavelength on coordination through azomethine nitrogen in the complexes [191].

The results obtained in this study justify the structure proposed to PbL_2 complexes. These results are the same as those found for the crystallographically determined structure and spectoscopically confirmed by Jang. [192].

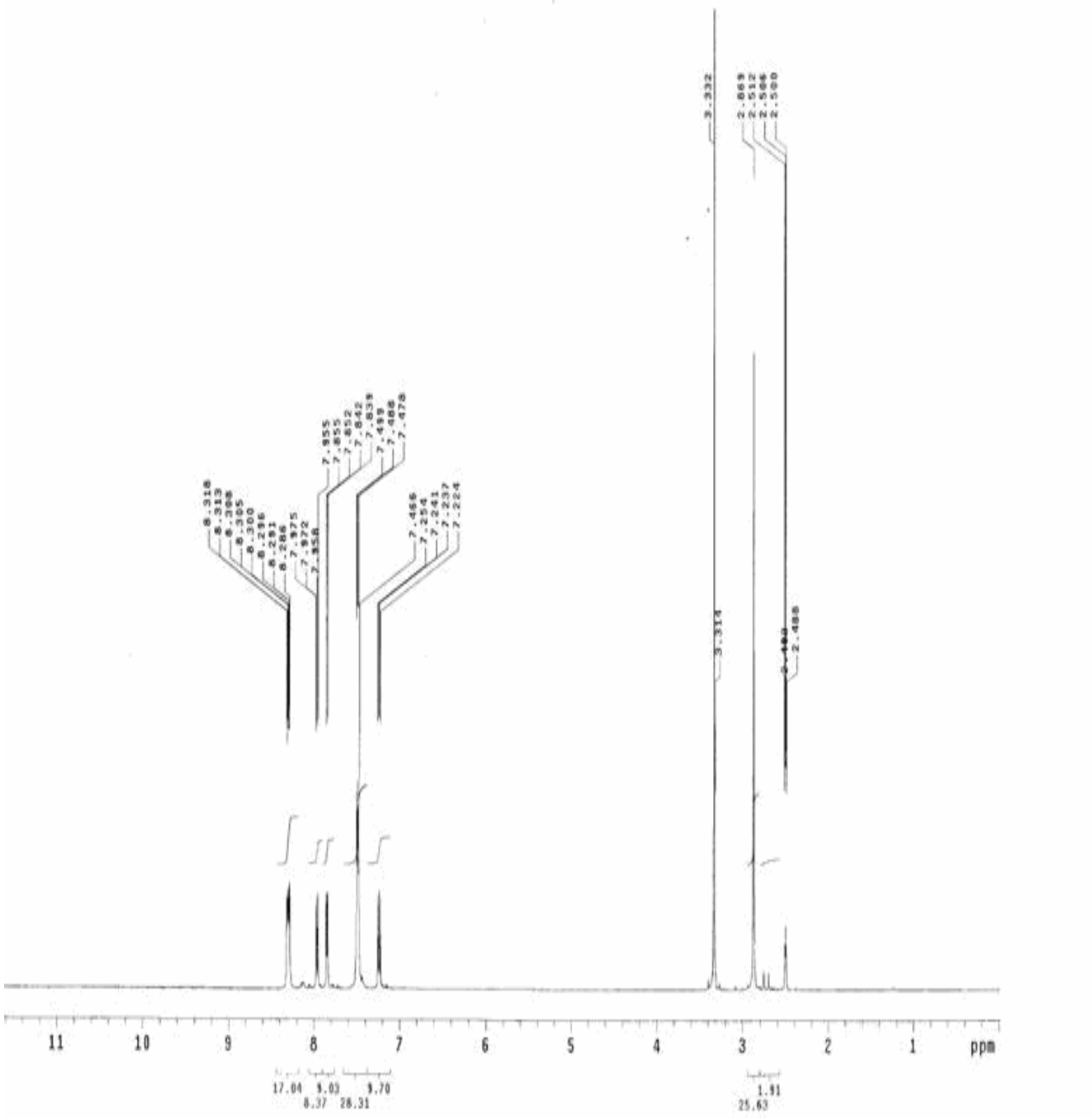

Figure (3.2). The ^{1}H-NMR spectrum of the complex $Pb(ATBH)_2$

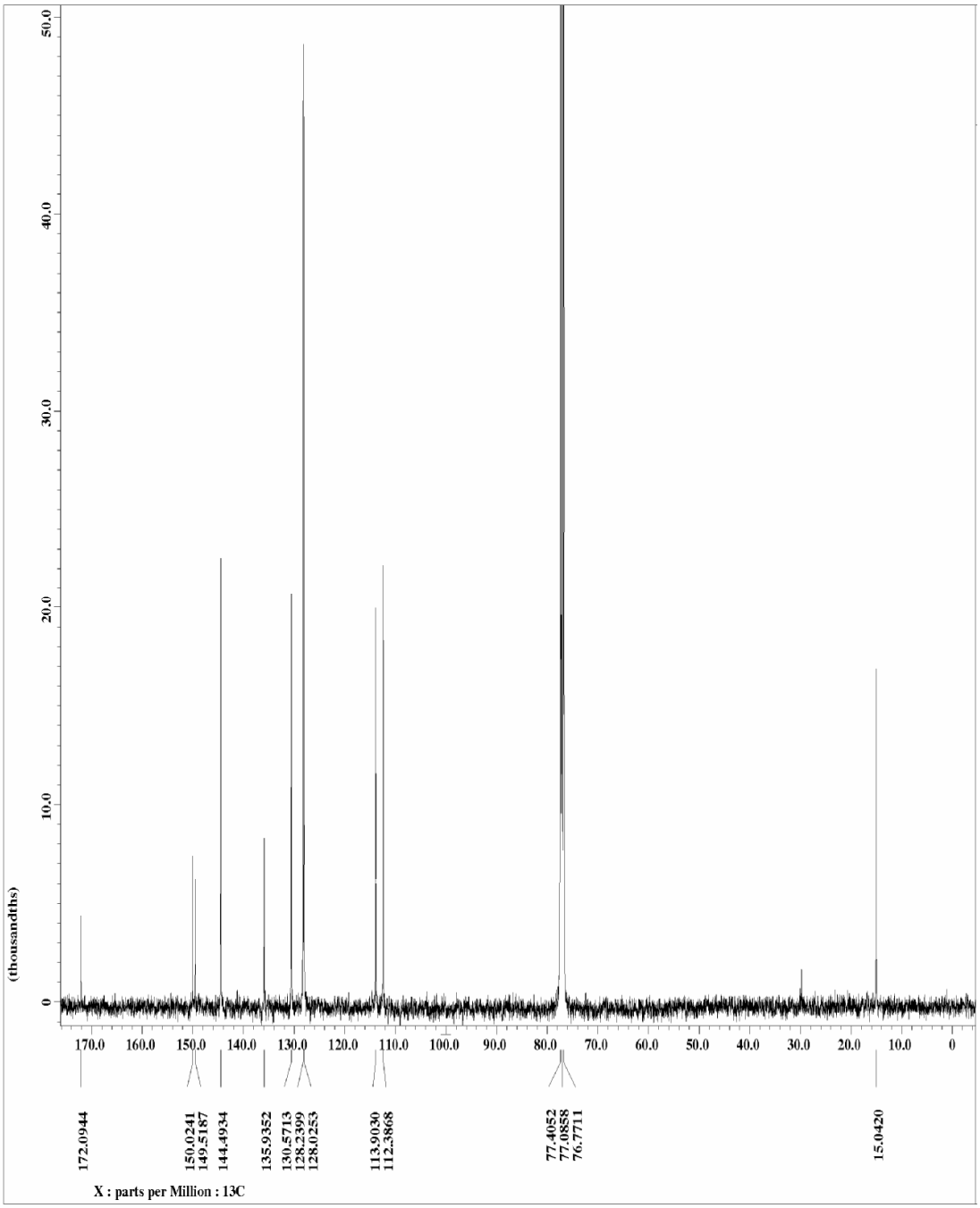

Figure (3.3). The ^{13}C-NMR spectrum of the complex $Pb(AFBH)_2$

3.2. Characteristics of the Electrodes

Ionophores used in ISEs should have rapid exchange kinetics and adequate formation constants in the paste. In addition, they should have good solublility in the paste matrix and sufficient lipophilicity to prevent dissolution from the paste into the sample solution [193]. The complexes, $Pb(ATBH)_2$ $Pb(CTBH)_2$ $Pb(AFBH)_2$ $Pb(CFBH)_2$, are almost insoluble in water making leaching ineffective and the complexes reasonable candidates as ionophores for lead ion-selective electrodes. A few electrodes individually comprising these complexes were constructed and tested to explore their effects as Pb(II) sensors $Pb(ATBH)_2$ was found the most sensitive and was characterized further to assess its proerties.

3.2.1. Effect of ionophore concentration on electrode potential

The influence of the amount of Pb(ATBH) as an ionophore on the potential response of the electrode was studied and the corresponding results are summarized in Table 3.1. The ionophore free electrode shows poor sensitivity to lead cations, sensor # 1, whereas the sensitivity of the electrodes response increased with increasing ionophore content. The best response was found at 0.5 wt% of the ionophore as indicated in sensor # 2 and sensor # 8. However, further addition of the ionophore resulted in a little decrease in the response of the electrode (in sensors #. 3-7 and # 9-13). This is most probably due to some inhomogenieties and possible saturation of the paste [194].

It is interesting to note that the graphite/plasticizer ratio of ca. 1.06 gave the best results with the optimum physical properties for sensor #2 and 1.18 for sensor #8 which ensured high enough mobilities of their constituents [195].

3.2.2. Plasticizer selection

Two parameters are of importance when manufacturing a carbon paste: (1) its mechanical stability and (2) its active surface area. Mechanical stability can be interpreted as the ability of the carbon paste to avoid erosion in solution. The use of plasticizers will give some permeable properties to the paste and will improve its mechanical stability by promoting binding between grains [196].

In addition, the solvent mediator (Plasticizer**)**, in particular, has a dual function: it acts as a liquifying agent, enabling homogenous solubilization and modifying the distribution constant of the ionophore used. The proportion of solvent mediator must be optimized in order to minimize the electrical asymmetry of the paste, to keep the sensor as clean as possible, and to stop leaching to the aqueous phase [197]. Therefore, for a plasticizer to be adequate in sensors, it should gather certain properties and characteristics such as having high lipophilicity, high molecular weight, low tendency for exudation from the paste matrix, low vapor pressure and high capacity to dissolve the substrate and other additives present in the paste [198].

In exploration for a suitable plasticizer for constructing this electrode, seven plasticizers where used in sample electrodes to figure out the plasticizer with the best response. These plasticizers have the following properties: dielectric constants, lipophilicity and molecular weight respectively listed in parantheses, namely, TPB (εr = 8.0, P_{TLC} = 4.0, M.wt. = 266), DOP (εr =5.1, P_{TLC} = 7.0, M.wt. = 391), DBP (εr = 6.4, M.wt. = 278), DOS (εr = 3.9, P_{TLC} = 10.1, M.wt. = 427), TEPh (εr = 4.8, P_{TLC} = 10.2, M.wt. = 434), 2-NPOE (εr = 23.6, P_{TLC} = 5.9, M.wt. = 251) and TCP (εr = 6.9, P_{TLC} = 5.9, M.wt. = 368), The CPE with DOS and TEPh as solvent mediators produced the best response, as shown in Figure 3.4. This is likely due to high lipophilicity, relatively high molecular

weight and low dielectric constant as well as ester groups that, in principle, are capable of interacting with cationic species; this plasticizer may solvate and adjust the mobility of ionophore. The results, given in Table (3.1), indicate that sensor #2 (48.3% TEph, 51.2% graphite and 0.5% ionophore) and sensor # 8 (45.5% DOS, 54.0% graphite and 0.5% Pb(ATBH)$_2$) give the best sensitivity, with a Nernstian slope of 27.1 and 28.2 mV/decade , detection limit of 3.9 x 10^{-7} M, 7.9 x 10^{-7} M over a relatively wide dynamic range of 5.9×10^{-7} – 1.0×10^{-2} M and $9.1x10^{-7}$ -1.0x 10^{-2} M of Pb(II) ions respectively. Therefore, these compositions were used to study various operation parameters of the electrode. The electrochemical performance characteristics of these electrode were systematically evaluated according to the International Union of Pure And Applied Chemistry (IUPAC) recommendations [199].

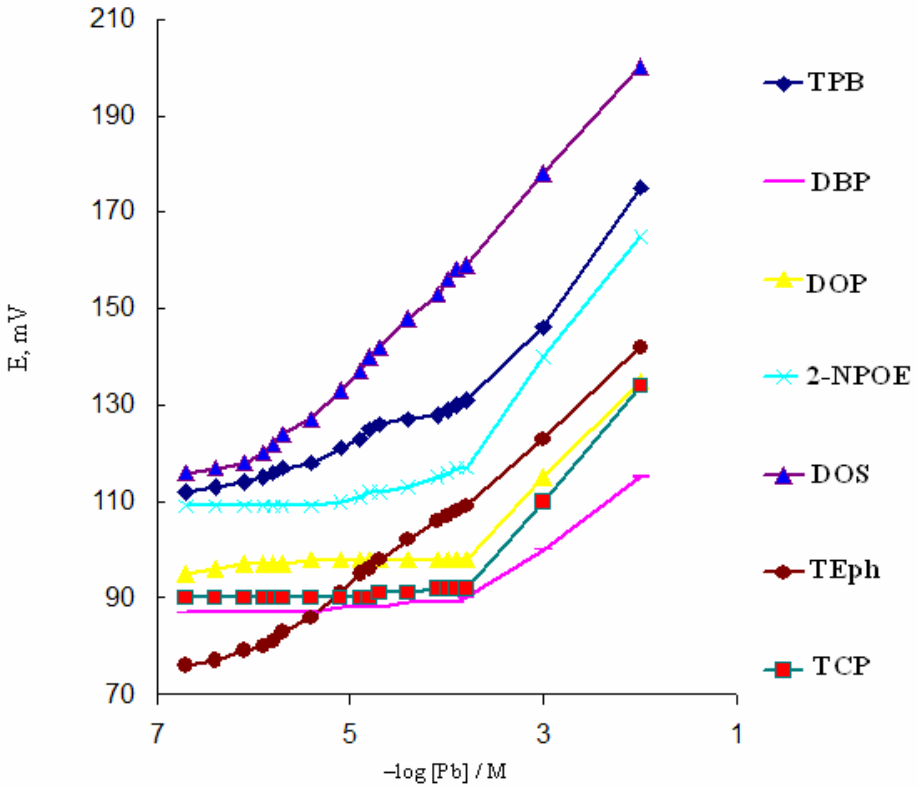

Figure (3.4) The effect of different plasticizers on lead electrode.

Table (3.1). Composition and slope of calibration curves for Pb-CMCPE electrodes at 25.0±0.1 °C.

Composition (%)					Electrode response			
Sensor	I-E	G	P		S	C.R.	LOD	$R_{(s)}$
L_1								
1-	--	54.4	45.6	TEph	13.2	$3.2x\ 10^{-4}$-$1.0\ x\ 10^{-2}$	$1.6x10^{-4}$	25-30
2-	0.50	51.2	48.3	TEph	27.1	5.9×10^{-7} – 1.0×10^{-2}	3.9×10^{-7}	5-8
3-	1.00	53.5	45.5	TEph	12.2	8.2×10^{-7}-$1.0x10^{-2}$	7.9×10^{-7}	10-12
4-	1.50	53.0	45.5	TEph	13.5	$7.9x10^{-7}$-$1.0x10^{-2}$	7.3×10^{-7}	9-13
5-	2.00	53.0	45.0	TEph	11.1	1.9×10^{-6}-$1.0x10^{-2}$	1.6×10^{-6}	12-15
6-	2.50	52.0	45.5	TEph	14.0	3.9×10^{-6}-$1.0x10^{-2}$	1.3×10^{-6}	8-9
7-	3.00	52.4	44.6	TEph	15.3	2.6×10^{-6}-$1.0x10^{-2}$	1.9×10^{-6}	9-13
8-	0.50	54.0	45.5	DOS	28.2	$9.1x10^{-7}$ -$1.0x\ 10^{-2}$	7.9×10^{-7}	5-10
9-	1.00	53.5	45.5	DOS	19.4	6.1×10^{-7}-$1.0x10^{-2}$	5.4×10^{-7}	8-11
10-	1.50	53.0	45.5	DOS	17.1	$7.9x10^{-7}$-$1.0x10^{-2}$	7.3×10^{-7}	10-13
11-	2.00	53.0	45.0	DOS	19.3	9.2×10^{-7}-$1.0x10^{-2}$	8.2×10^{-7}	9-12
12-	2.50	52.0	45.5	DOS	18.6	2.2×10^{-6}-$1.0x10^{-2}$	1.9×10^{-6}	8-13
13-	3.00	52.4	44.6	DOS	18.1	3.1×10^{-6}-$1.0x10^{-2}$	1.9×10^{-6}	8-12
Different of complexes								
14- L_2	0.50	51.2	48.3	TEph	10.2	$1.1x10^{-7}$-$1.0x10^{-3}$	9.3×10^{-7}	10-14
15- L_3	0.50	51.2	48.3	TEph	26.1	$1.25x10^{-6}$-$1.0x10^{-3}$	1.9×10^{-6}	8-12
16- L_4	0.50	51.2	48.3	TEph	16.6	$2.9x10^{-6}$-$1.0x10^{-2}$	1.1×10^{-6}	7-13
17- L_2	0.50	54.0	45.5	DOS	13.1	$2.5x10^{-6}$ -$1.5x10^{-4}$	4.9×10^{-6}	10-13
18- L_3	0.50	54.0	45.5	DOS	10.3	$3.2x10^{-6}$ -$1.0x10^{-3}$	2.2×10^{-6}	9-12
19- L_4	0.5 0	54.0	45.5	DOS	12.2	$1.6x10^{-6}$-$1.0x10^{-3}$	8.9×10^{-7}	10-14
Different plasticizers plasticizers								
(2-NPOE)	0.48	54.1	45.5		25.0	$3.9x10^{-5}$-$1.0x10^{-2}$	1.3×10^{-5}	12-15
(DOP)	0.48	54.1	45.5		20.3	$2.2x10^{-4}$-$1.0x10^{-2}$	$1.6x10^{-4}$	5-8
(DBP)	0.48	54.1	45.5		15.2	$3.0x10^{-4}$-$1.0x10^{-2}$	$1.6x10^{-4}$	9-14
(DOS)	0.48	54.1	45.5		28.2	$9.1x10^{-7}$ -$1.0x10^{-2}$	7.9×10^{-7}	5-10
(TCP)	0.48	54.1	45.5		24.0	$2.2x10^{-4}$-$1.0x10^{-2}$	$1.6x10^{-4}$	10-14
(TEPh)	0.50	51.2	48.3		27.1	5.9×10^{-7} – 1.0×10^{-2}	3.9×10^{-7}	5-8
(TBP)	0.50	54.0	45.5		22.4	$1.6x10^{-6}$ -$1.0x\ 10^{-2}$	1.2×10^{-6}	12-15
Different g/p ratios for sensor #2								
0.85	0.50	45.8	53.7	TEph	22.1	8.9×10^{-7} – 1.0×10^{-2}	8.2×10^{-7}	8-10
0.95	0.50	48.5	51.0	TEph	21.5	$9.5x10^{-7}$ – 1.0×10^{-2}	7.3×10^{-7}	12-15
1.06	0.50	51.2	48.3	TEph	27.1	5.9×10^{-7} – 1.0×10^{-2}	3.9×10^{-7}	5-8
1.18	0.79	53.9	45.4	TEph	25.3	$8.1x10^{-7}$-$1.0x10^{-3}$	7.9×10^{-7}	13-15
1.25	0.50	55.4	44.1	TEph	24.1	$9.3x10^{-7}$ -$1.0x10^{-3}$	8.1×10^{-7}	9-14
1.35	0.60	57.1	42.3	TEph	25.2	$1.9x10^{-6}$-$1.0x10^{-2}$	8.9×10^{-7}	10-12
1.45	0.64	58.8	40.6	TEph	26.2	$2.1x10^{-6}$-$1.0x10^{-2}$	1.2×10^{-6}	10-13
Different g/p ratios for sensor #8								
0.85	0.50	45.8	53.7	DOS	16.3	9.9×10^{-7} – 1.0×10^{-2}	8.2×10^{-7}	10-12
0.95	0.50	48.5	51.0	DOS	13.5	1.9×10^{-6} – 1.0×10^{-2}	1.2×10^{-6}	8-12
1.06	0.50	51.2	48.3	DOS	21.1	$2.1x10^{-6}$-$1.0x10^{-2}$	1.5×10^{-6}	8-10
1.18	0.47	54.1	45.5	DOS	28.2	$9.1x10^{-7}$ -$1.0x10^{-2}$	7.9×10^{-7}	5-8
1.25	0.50	55.4	44.1	DOS	17.0	$2.9x10^{-6}$-$1.0x10^{-2}$	1.9×10^{-6}	10-12
1.35	0.60	57.1	42.3	DOS	18.3	$2.7x10^{-6}$-$1.0x10^{-2}$	2.0×10^{-6}	9-13
1.45	0.64	58.8	40.6	DOS	19.1	$1.9x10^{-6}$-$1.0x10^{-2}$	1.7×10^{-6}	10-15

I.P: Ion-pair, S: slope (mV/decade), C.R.: concentration range (M), LOD: limit of detection, $R_{(s)}$: response time(s), P: Plasticizers (TEph, DOS).
L_1: $Pb(ATBH)_2$, L_2: $Pb(CTBH)_2$, L_3: $Pb(AFBH)_2$, L_4: $Pb(CFBH)_2$

3.2.3 Selectivity coefficients

Selectivity is an important characteristic of a sensor that delineates the extent to which the device may be used in estimation of the analyte ion in presence of other ions and the extent of utility of any sensor in real sample measurement [200].

The effect of the interfering ions on the response behavior of the sensors #2 and #8 was evaluated by the separate solution method (SSM). As can be seen from Table(3.2), most ions have negligible interference. However, Cu(II) shows intermediate effect, which is likely due to the marked ability of copper(II) to form distorted octahedral complexes

Table 3.2. Selectivity coefficient for Pb-CMCPEs

Interfering ions	Selectivity coefficients (K)	
	Sensor #2	Sensor #8
Na^{+}	1.21 X 10^{-4}	8.61 X10^{-2}
NH_4^{+}	1.28 X 10^{-4}	2.82 X10^{-3}
K^{+}	2.27 X 10^{-2}	1.34 X10^{-2}
Li^{+}	4.64 X 10^{-3}	2.44 X 10^{-3}
Co^{2+}	3.16 X 10^{-5}	2.45 X 10^{-4}
Cd^{2+}	8.25 X 10^{-6}	2.10 X 10^{-5}
Ca^{2+}	1.00 X 10^{-6}	3.81 X 10^{-5}
Zn^{2+}	1.21 X 10^{-6}	2.83 X 10^{-5}
Mg^{2+}	1.46 X 10^{-6}	1.48 X 10^{-6}
Ba^{2+}	1.09 X 10^{-5}	4.75 X 10^{-5}
Cu^{2+}	3.16 X 10^{-1}	1.56 X 10^{-2}
Al^{3+}	3.16 X 10^{-7}	1.95 X 10^{-4}
Ce^{3+}	1.45 X 10^{-5}	4.41 X 10^{-5}

3.2.4 Effect of acidity

The influence of the pH on the response of the carbon paste electrode was studied at 1.0 x 10^{-5} M lead(II) ion in the pH range of 2.0–10.5. The pH was adjusted by 0.1 M solutions of hydrochloric acid or sodium hydroxide. It can be seen from Figure 3.5 that the variation in potential is acceptable in the pH range 5.8–7.6. Under more acidic conditions, the response to hydronium ion may become pronounced as its concentration increases exponentially on lowering the pH of the solution. The drift in potential at pH 7.6 is attributed to formation of lead(II) hydroxide.

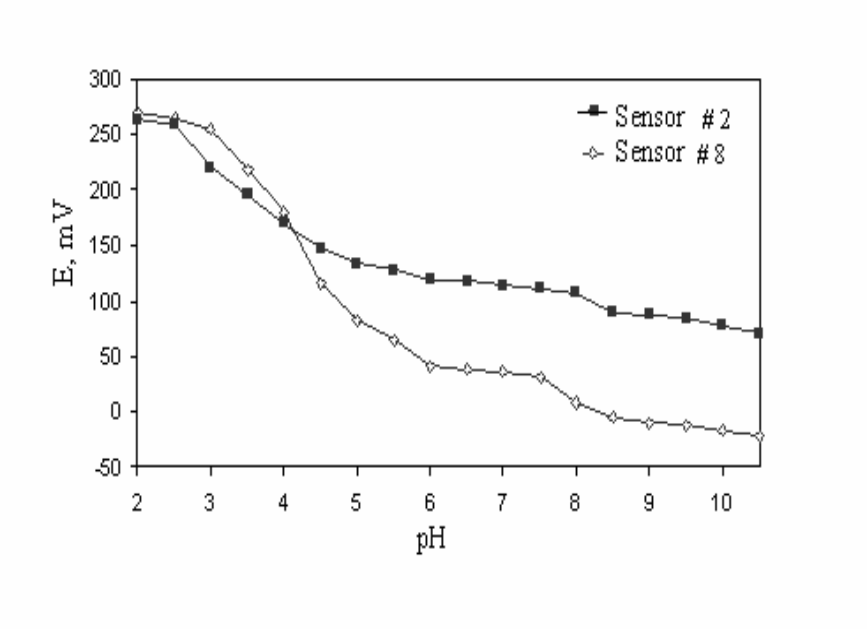

Figure (3.5) Effect of pH on the response of sensors # 2 and # 8 at 1.0 x 10^{-5} M lead(II) ion

3.2.5 Dynamic response time, renewal surface and reproducibility of the electrodes

The response time of the electrodes was obtained by measuring the time required to achieve a steady state potential (within ±1 mV) after successive immersion of the electrodes in a series of Pb(II) solutions, each having a 10-fold increase in concentration from 1.0×10^{-5} to 1.0×10^{-2} M. The electrodes yielded steady potentials within 5–8 s (as shown in Figure 3.6 and 3.7) [35]. The potential reading stays constant, to within ±1 mV, for at least 5 min. To evaluate the reversibility of the electrode, the electrode potential was measured alternatively in various solutions containing 1.0×10^{-4} M and 1.0×10^{-5} M as shown in Figure 3.8 which clearly indicates that equilibrium is reached in a very short time (~8 s). The response characteristics of the electrodes were systematically evaluated according to the IUPAC recommendations [199] and summarized in Table (3.1). The repeatability of the potential reading for each electrode was examined by subsequent measurement in 1.0×10^{-3} M solution immediately after measuring the first set of solutions at 1.0×10^{-4} M. The standard deviation of the measured electromotive force (emf) for five replicate measurements obtained are 1.03, 1.38 for electrodes # 2 and # 8 in 1.0×10^{-4} M solution, and 0.35, 0.55 in 1.0×10^{-3} M solution respectively. This indicates excellent repeatability of the potential response of the electrodes.

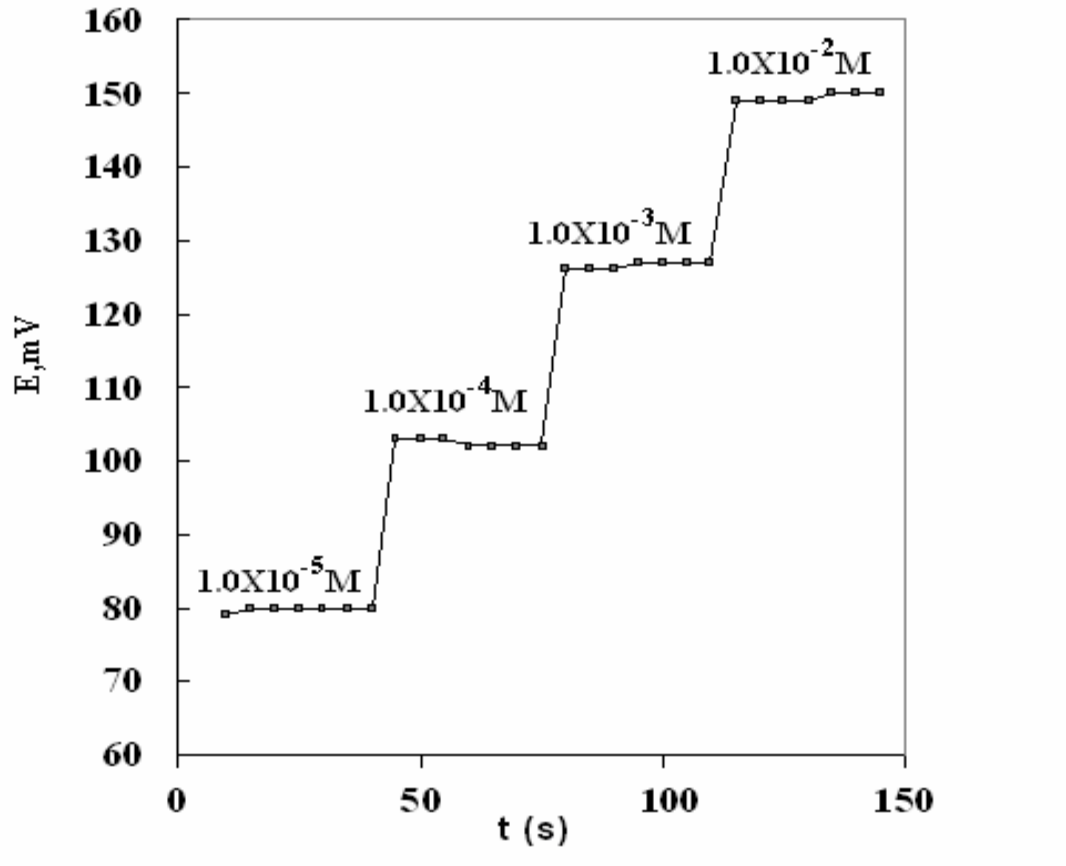

Figure (3.6) Dynamic response of sensors # 2

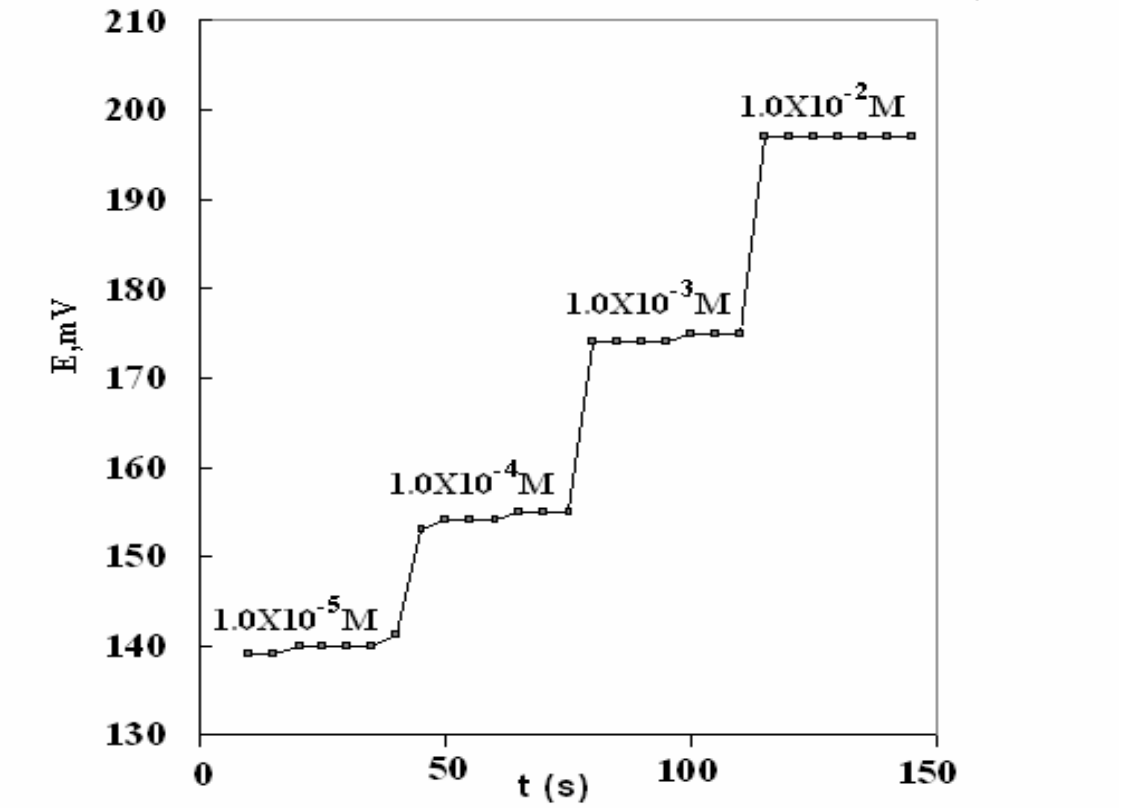

Figure (3.7) Dynamic response of sensors # 8

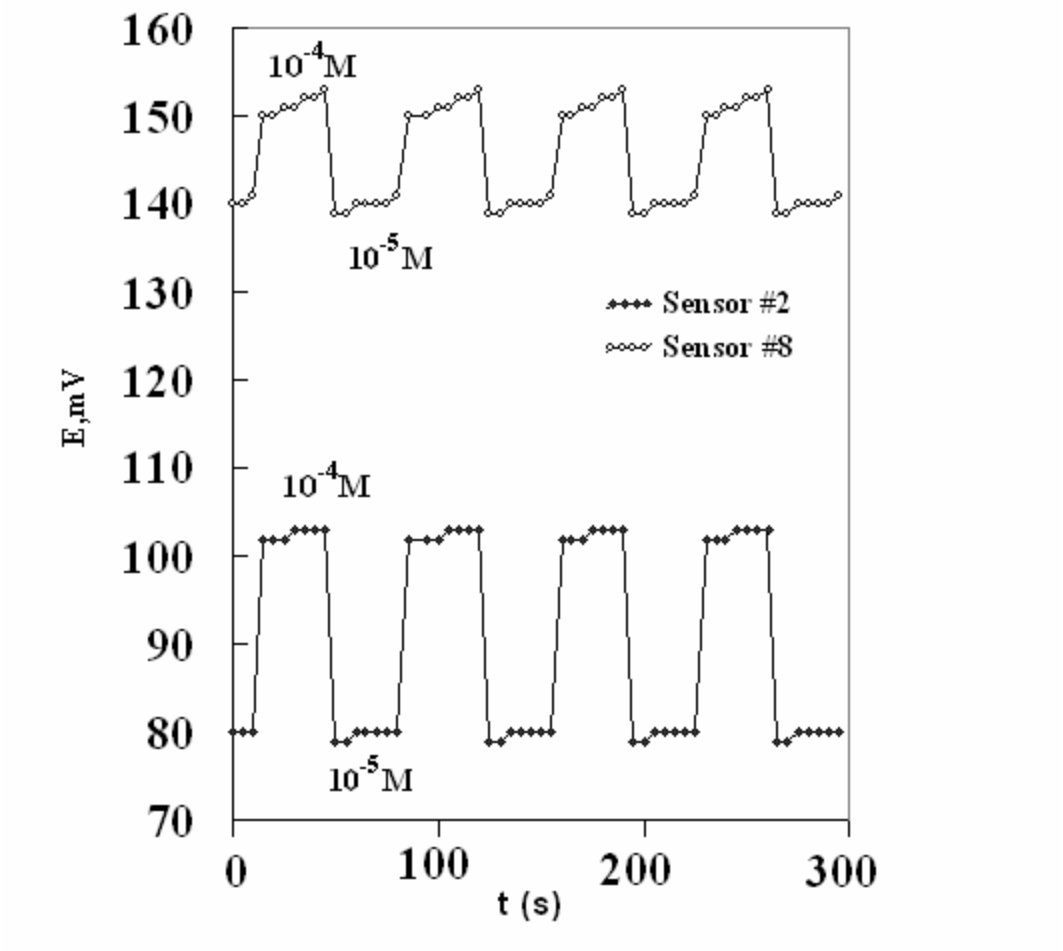

Figure (3.8) Dynamic response of sensors # 2 and # 8 for alternate measurements

3.2.6 Effect of temperature

To study the thermal stability of the electrodes, calibration curve ($E_{electrode}$ Potential, $E_{elect.}$ vs pPb) were constructed at different temperatures 20-50 ^{o}C. The slope and usable concentration range, detection limit and response time of the electrode at different temperatures are given in Table (3.3) for Pb- CMCPEs. The results indicate that the slopes of the calibration curves were slightly affected by the increase of the temperature of the test solutions up to 50^{o}C.

Table (3.3) Performance characteristics of sensor #2 and sensor #8 electrodes at different temperature

Pb- CMCPEs	Temperature (^oC)	Slope (mV/decade)	Concentration range (M)	Detection Limit (M)	Response time (Sec.)
Sensor#2					
	20	26.9	$6.2x10^{-7}$-$1.0x10^{-2}$	$4.0x10^{-7}$	6-9
	25	27.0	5.9×10^{-7}-$1.0x10^{-2}$	3.9×10^{-7}	5-8
	30	27.5	$6.0x10^{-7}$-$1.0x10^{-2}$	$4.2x10^{-7}$	8-10
	35	27.0	$5.9x10^{-7}$-$1.0x10^{-2}$	$4.2\ x10^{-7}$	7-9
	40	26.0	$6.3x10^{-7}$-$1.0x10^{-2}$	$5.0x10^{-7}$	8-11
	45	26.5	$6.0\ x10^{-7}$-$1.0x10^{-2}$	$5.2\ x10^{-7}$	8-11
	50	26.8	$6.4x10^{-7}$-$1.0x10^{-2}$	$5.4x10^{-7}$	9-12
Sensor#8					
	20	27.5	$9.3x10^{-7}$-$1.0x10^{-2}$	$8.0x10^{-7}$	6-9
	25	28.0	$9.1x10^{-7}$-$1.0x10^{-2}$	7.9×10^{-7}	5-10
	30	28.0	$9.4x10^{-7}$-$1.0x10^{-2}$	$8.3x10^{-7}$	7-11
	35	27.2	$9.2x10^{-7}$-$1.0x10^{-2}$	$7.9x10^{-7}$	6-10
	40	27.3	$9.0x10^{-7}$-$1.0x10^{-2}$	$8.2x10^{-7}$	8-11
	45	27.0	$9.4x10^{-7}$-$1.0x10^{-2}$	$8.2x10^{-7}$	9-13
	50	27.6	$9.3x10^{-7}$-$1.0x10^{-2}$	$8.4x10^{-7}$	8-13

3.3. Response of the Electrode Based $Pb(ATBH)_2$ to Lead (II) Ions

Potentiometric response of sensors #2 and #8 was tested for different cations such as Na^+, K^+, NH_4^+, Li^+, Mg^{2+}, Cd^{2+}, Ba^{2+}, Ca^{2+}, Cu^{2+}, Zn^{2+}, Co^{2+}, Ce^{3+} and Al^{3+} . As can be seen from Figures 3.9 and 3.10 the slopes of the linear parts of the potential responses of the sensors #2 and #8 for most of the tested cations are much lower than those expected by the Nernst equation. However, Pb^{2+} has the closest Nernstian response over a wide concentration range with low detection limit.

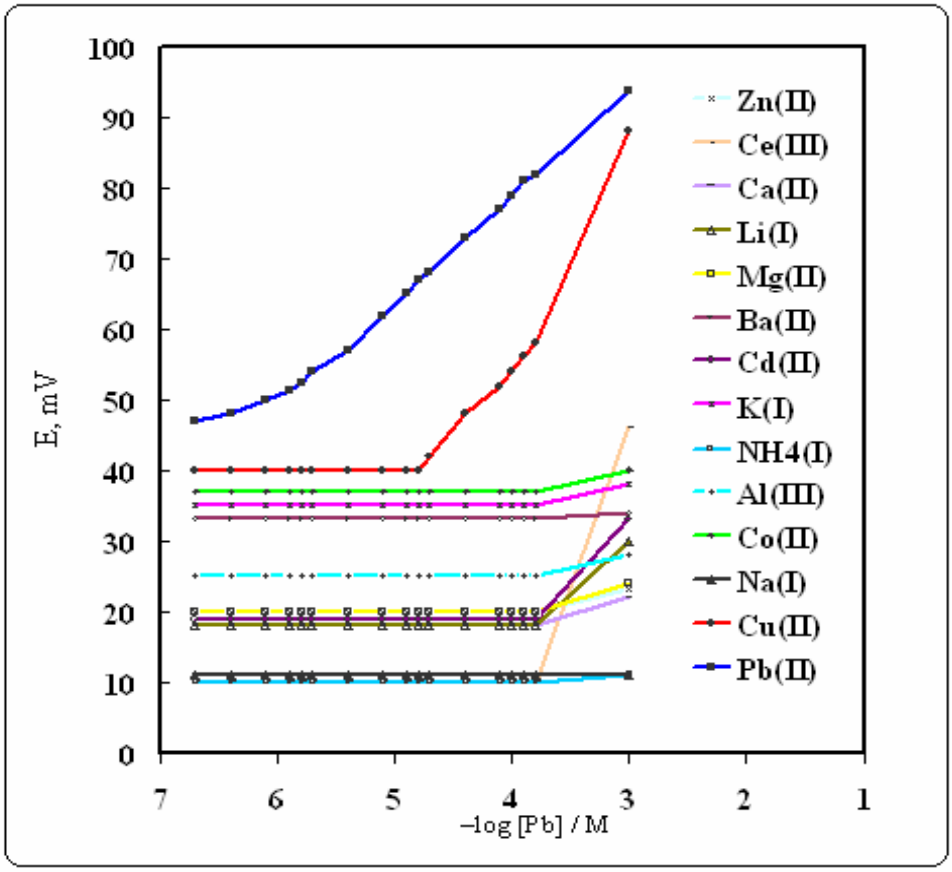

Figures (3.9) Potential response of various metal ions for sensor # 2

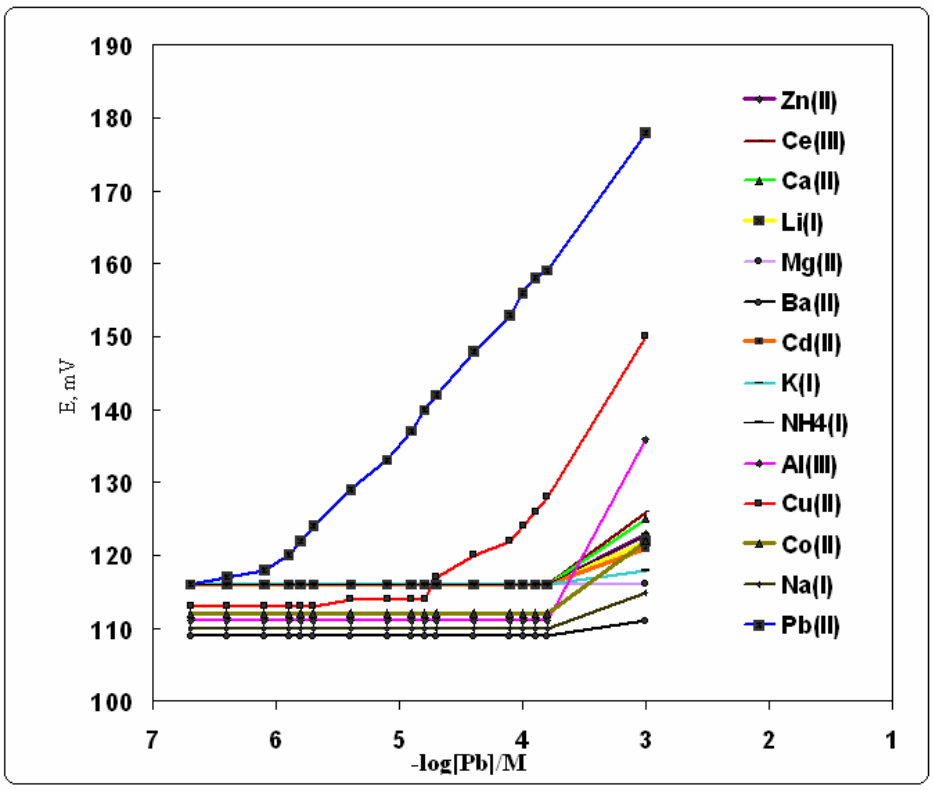

Figures (3.10) Potential response of various metal ions for sensor # 8

3.4. Analytical Applications

The proposed sensors were found to work well under laboratory conditions. It is clear that the amount of Pb(II) ions can be accurately determined using these electrodes.

3.4.1. Potentiometric determinations

3.4.1.1. The potentiometric titration method

The potentiometric titration of lead ion is based on the decrease of the lead cation concentration by precipitation with EDTA. The feasibility of such titration depends on the degree of completeness of the reaction.

The sensors were successfully applied as an indicator electrodes in potentiometric titration in aqueous solution containing 1.035 to 14.5 mg of lead ion. Typical results of titration of Pb(II) are shown in Figure (3.11) and (3.12). The added titrant caused a decrease in potential as a result of a decrease in free Pb(II) ion due to formation of a complex with EDTA. The amount of Pb(II) ions in solutions can be accurately determined from the resulting titration curves.

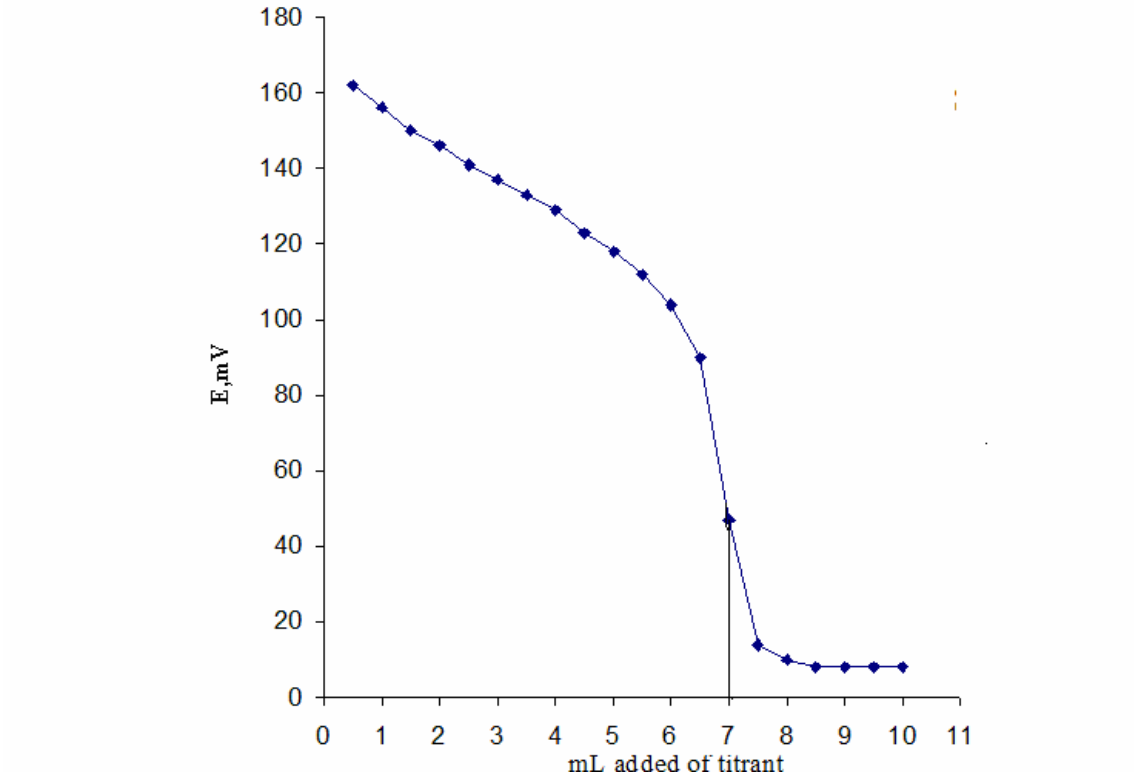

Figure (3.11) Potentiometric titration curve of 7.0 ml of 1.0×10^{-3} M (1.4mg) solution of Pb(II) with 1.0×10^{-3} M EDTA using sensors #2.

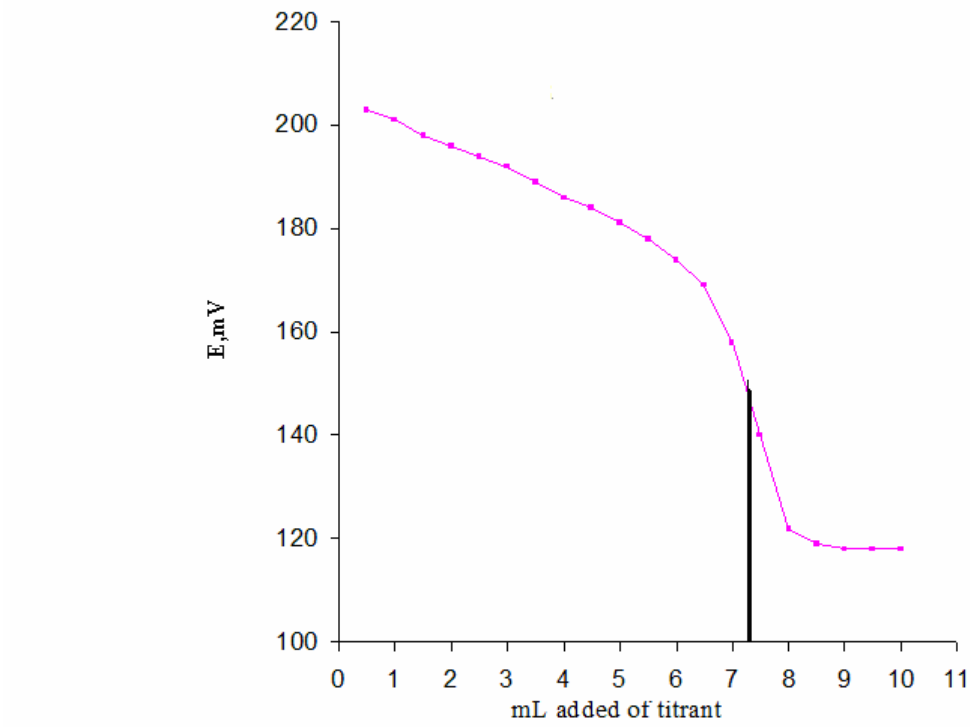

Figure (3.12) Potentiometric titration curve of 7.0 ml of 1.0×10^{-3} M (1.4mg) solution of Pb(II) with 1.0×10^{-3} M EDTA using sensors #8

3.4.1.2. The standard additions method

Lead ion were determined by the standard additions method. The results, shown in Table (3.4), indicate that recovery ranged from 99.0%-96.8% and small relative standard deviation ranging from 1.77-2.66% in lead ion. These values reflect high accuracy and precision of the studied electrodes as sensors for the lead complexes.

3.4.1.3. The calibration curve method

A calibration curve is a general method for determination of the concentration of a substance in an unknown sample by comparing the response of the unknown to those of a set of standard samples of known concentration. Lead ion was determined by the calibration curve method. The results, shown in Table 3.4, indicate that recovery ranged from 98.5%-101.5% and small relative standard deviation ranging from 0.92-0.38% for lead complexes. The accuracy and precision of these findings indicate the viability of these electrodes in lead ion determination.

Table (3.4). Analysis of lead(II) in double distill water samples using different methods

Methods	M		X	R.S.D%
	Taken	Found		
		Sensor #2		
Standard additions				
	1.00×10^{-6}	1.01×10^{-6}	101.0%	2.15
	5.00×10^{-6}	4.95×10^{-6}	99.0%	1.77
	5.00×10^{-5}	4.84×10^{-5}	96.8%	2.66
Calibration curve				
	1.99×10^{-6}	1.96×10^{-6}	98.5%	0.92
	1.99×10^{-5}	2.02×10^{-5}	101.5%	0.38
	1.00×10^{-3}	1.00×10^{-3}	100.0%	0.85
		Sensor #8		
Standard additions				
	5.00×10^{-6}	4.91×10^{-6}	98.2%	1.81
	5.00×10^{-5}	4.88×10^{-5}	97.6%	1.97
	1.00×10^{-6}	1.01×10^{-5}	101.5%	0.97
Calibration curve				
	1.99×10^{-6}	1.95×10^{-6}	97.9%	0.91
	1.96×10^{-5}	1.99×10^{-5}	101.5%	0.43
	1.00×10^{-3}	1.01×10^{-3}	101.5%	0.63

The number of replicate measurements = 4

X : recovery, R.S.D. relative standard deviation.

CONCLUSIONS

A number of new lead(II) complexes, PbL_2 with some trifunctional SNO-donor and ONO-donor atoms have been synthesized and characterized on the basis of elemental analysis, molar conductances and spectroscopic (electronic, IR, ^{1}H-NMR, and ^{13}C-NMR) data. The ligands behave as monobasic tridentate, bonding to the metal(II) ion through the acetylthiophene ring sulfur or acetylfuran ring oxygen, azomethine nitrogen, and benzoyl oxygen to form distorted octahedral structures where the deprotonated form is preferred in the coordination. $Pb(ATBH)_2$ was found a suitable ionophore in a lead(II)-CPE. It was utilized in fabrication of two electrodes where TEph and DOS were efficient plasticizers and the electrodes were fully characterized. Their detection limit were 3.9×10^{-7} M, 7.9×10^{-7} M, concentration range 5.9×10^{-7} –1.0×10^{-2} M, 9.1×10^{-7} -1.0×10^{-2} M response time ~ 8-10 sec and acceptable pH range was 5.8-7.6. The modified electrodes were applied as an indicator electrode and successfully used to determine Pb(II) in drinking water samples giving satisfactory results.

REFERENCES

1) J. E. House. *Inorganic Chemistry*, Printed in Canada, Academic Press is an imprint of Elsevier, (2008).

2) F. A. Cotton, G. Wilkinson and P. L. Gaus, *Basic Inorganic Chemistry*, 3rd, John wiley and sons, Inc, Canada, (1995).

3) J. E. Huheey, E. A. Keiter and R. L. Keiter, *Inorganic Chemistry*, 4th ed, HarperCollins, New York, (1993).

4) C. E. Housecroft and A. G. Sharp, *Inorganic Chemistry*, 2nd ed, Printed by Ashford Colour Press Ltd., Gosport, Pearson Education, (2005.

5) R. H. Crabtree, *The organometallic chemistry of the Transition Metal*, 3rd ed., Wiley-Interscience, (2001).

6) D. Harris, and M. Bertolucci, *Symmetry and Spectroscopy*, New York, Dover Publications, (1989).

7) G. L. Miessler and D. A. Tarr, *Inorganic Chemistry*, 3rd ed., Pearson education, (2004).

8) R. Change, *General Chemistry* , 3rd ed, McGraw-hill, New YORK, (2003).

9) D. F. Shriver, P. W. Atkins and C. H. Langford, *Inorganic Chemistry* ,2nd ed., Oxford University Press, (1990).

10) A. von Zelewsky, *"Stereochemistry of Coordination Compounds"* John Wiley: Chichester, (1995).

11) C. J. jones, *d- and f- Block chemistry* , Royal Society of chemistry , (2002)

12) F. Hueso-Urena, N. Illan-Cabeza, A. Moreno-Carretero, M..N, Penas Chamora, A. L, *Acta Chem. Solv.*, 47, 487 (2000).59 (1993).

13) E. Colacio, M. Ghazi, R. Kivekias, M. Klinga, F. Lioret, J. M. Moreno, *Inorg. Chem*., 39, 2772-2775(2002).

14) A. R. S. Ferwanah, A. M. Awadallah, B. M. Awad, N. M. El-Halabi and R. Boese, *Inorganica Chimica Acta* 358, 4511-4518 (2005).

15) Z, Steven S. *Chemical Principles*, 5th ed. New York: Houghton Mifflin, 2005..

16) N. M. El-Halabi, A. M. Awadallah, W M. Faris, K. Seppelt and H. Shorafa, *The Islamic University Journal (Series of Natural Studies and Engineering),* 17, 1-10 (2009).

17) M. Shebl, *Spectrochimica Acta Part A*, 73, 313 (2009).

18) S. A. Patil, V. H. Naika, A. D. Kulkarnia, P. S. Badamib *Spectrochimica Acta Part A*, 75, 34, (2010).

19) A. Lewenstam, M. Maj-Zurawska, A. Hulanicki, *electroanalysis*, 3, 727 – 734 (1991).

20) H. M. Abu-Shawish, *electroanalysis*, 20,491 – 497(2008).

21) H. Ibrahim, Y. M. Issa and H. M. Abu-shawish, *Anal. Chim. Acta*, 532, 79 (2005).

22) M. M. Khater, Y. M. Issa and S. H. Mohammed, *Bioelect. chem*, 77, 53 (2009).

23) H. M. Abu-shawish and S. M. Saadeh, Can. J. *Anal. Chem*., 52, 225 (2007).

24) E. Bakker and K. K. Torres, J. Braz. *Chem. Soc*., 19, 621 (2008).

25) R. P. Buck and E. Linder, *Anal. Chem*., 73,88 (2001).

26) E. Lindner, Z. Niegreisz, K. Toath, E. Pungor, T. Berube and R. Buck, J. *Electroanal. Chem*., 259, 67(1989).

27) R.D. Braun, *"Introduction to Instrumental Analysis"*, 19th ed, McGraw-Hill, New York (1987).

28) D. Wstone and D. Yee, *Electrochim. Acta.*, 16, 549 (1971).

29) E. Csoregi, L. Gorton and G. Marko-Varga, *Anal. Chim. Acta*., 273, 59 (1993).

30) W. E. Morf, E. Linder and W. Simon, *Anal. Chem.*, 47, 1596 (1975).

31) C. Gavach and C. Bertrand, *Anal. Chim. Acta.*, 55, 385 (1971).

32) G.G. Guilbault, *Pure Apple. Chem.*, 25,72 (1971).

33) D. C. Cowel and P. A. E. Ford, *Clin. Chem*., 33,145 (1987).

34) D. M. Pranitis and M. E. Meyerhoff, *Anal. Chem.*, 59, 2345 (1987).

35) R. L. Solsky, *Anal. Chem.*, 60,106 (1988).

36) T. Fonong, *Anal. Chim. Acta.*, 186,301 (1986).

37) P. Bergveld, Iee Trans. *Biomed. Eng.*, 19,342 (1972).

38) J. Janata, *Analyst*, 119,2275 (1994).

39) D. M. Band and T. Treasure, *"Ion-Selective Electrode Methodology II"* , 41 (1979).

40) J. Wang, *"Analytical Electrochemistry"*, VCH, New York (1994).

41) P. D. Beer and R. J. Mortimer, N.R. Stradiotto, F. Szemes and J. S. *Weightman, Anal. Proc.*, 32,419 (1995).

42) E. Bkker and E. Pretsch, *Anal. Chem*., 74, 420 (2002).

43) W. E. Morf and W. Simon, *Chem.*, 1, 211 (1978).

44) D. Amman, W. E. Morf, P. Anker, P. C. Meier, E. Pretsch and W. Simpn, *Selective Electrode Revs.*, 5, 3 (1983).

45) M. S. Frant, *Analyst*, 119, 2293 (1994).

46) T. P. Byrne, *Selective Electrode Revs.*, 10, 107 (1988).

47) M. S. Frant, *Analyst*, 119, 2293 (1994).

48) K. Vytras, M. Dajkova and M. Remes. *Cesk farm*, 30, 61 (1981).

49) R. W. Cattral and I.C. Hamilton, *Ion Sel. Electrode Rev*.,6, 125 (1984).

50) I. Svancara, K. Vytras, J. Barek and J.Zima, *CRAC*, 31,311 (2001).

51) I. Svancara, K. Vytras, K. Kalcher, A. Walcarius and J. Wang, *Electroanalysis*, 21, 7 (2009).

52) K. Kalcher, I. Svancara, R. Metelka, K. Vytras and A. Walcarius, Heterogeneous carbon electrochemical sensors. In Encyclopedia of Sensors, Grimes, C.A., Dickey, E.C. and Pishko, M.V. (eds.), American Scientific Publishers: Stevenson Ranch, CA, USA, 4, 283–429 (2006).

53) P. T. Kissinger and W. R. Heineman, *Laboratory Techniques in Electroanalytical Chemistry*, 2nd ed.; Marcel Dekker: New York (1996).

54) J. Wang, *Analytical Electrochemistry*, Wiley-VCH: New York (2000).

55) I. Svancara, K. Vytras, J. Barek, and J. Zima , *Anal. Chem*., 31, 311 (2001).

56) H. M. Abu-Shawish, S. M. Saadeh, *Sens. Lett.*, 5, 559 (2007).

57) P. Fanjul-Bolado, D. Hernandez-Santos, P.J. Lamas-Ardisana, A. Martın-Pernıa and A. Costa-Garcıa, *Electrochim. Acta.,* 53, 3635 (2008).

58) K. Vytras, I. Svancara and R. Metelka, J. Serb. *Chem. Soc.*, 74, 1021 (2009).

59) I. Svancara1, A.Walcarius, K. Kalcher and K. Vytras1, *Cent. Eur. J. Chem*. ,7(4) , 598 (2009).

60) I. Svancara, J. Konvalina, K. Schachl, K. Kllacher and K.Vaytras, *Electroanalysis*, 10, 435 (1998).

61) Z. Q. Zhang, H. Lui, H. Zhang and Y. F. Li., *Anal. Chem. Acta.,* 333 ,119 (1996).

62) I. Svancara, K .Kalcher, W .Diewald and k. Vytras, *Electroanalysis*, 8,336 (1996).

63) F. Faridbod, M. R. Ganjali, R. Dinarvand and P. Norouzi, Afr. J. *Biotechnol.*, 6, 2960 (2007).

64) P. R. Buck, E. Lindner, *Pure Appl. Chem.*, 66, 2527 (1994).

65) L. A. Currie and G. Svehla, *Pure & Appl. Chem.*, 66, 595 (1994).

66) K. Danzer, L. A. Curriet. *Guidelines for Calibration in Analytical Chemistry. Pure &Appl. Chem.,*. 70, 993 (1998).

67) J.S. Casas, J. Sordo (Eds.), *Lead: Chemistry, Analytical Aspects, Environmental Impact and Health Effects*, Elsevier, 2006.

68) B.T. Farrer, V.L. Pecoraro, Curr. *Opin. Drug Discov. Dev.*, 5, 937 (2002).

69) E.S. Claudio, H. A. Godwin, J. S. Magyar, *Progr. Inorg. Chem.*, 51, 1 (2003).

70) G. Saxena, S.J.S. Flora, J. Biochem. *Mol. Toxicol.*, 18, 221(2004).

71) R. C. Gracia,W. R. Snodgrass, *Am. J. Health Syst. Pharm*. 64, 45(2007).

72) J. S. Magyar, T .C.Weng, C. M. Stern, D. F. Dye, B. W. Rous, J.C. Payne, B. M. Bridgewater, A. Mijovilovich, G. Parkin, J. M. Zaleski, J. E. Penner-Hahn, H. A. Godwin, J. Am. *Chem. Soc.*, 127, 9495(2005).

73) G. M. Hettiarachchi, G. M. Pierzynski, *Environ. Progr*., 23, 78(2004).

74) S. K. Khatik, R. Thakur, G.D. Sharma, *J. Ind. Pollut. Control* 22, 233(2006).

75) A. V. Mudring, Stereochemical activity of lone pairs in heavier main-group element compounds, in: G.Meyer, D.Naumann, L.Wesemann (Eds.), *Inorganic Chemistry in Focus*, vol. III,Weinheim, p. 15, (2006).

76) A.Walsh, G.W.Watson, *J. Solid State Chem*., 178, 1422(2005).

77) N. A. Spaldin,W. E. Pickett, *J. Solid State Chem*., 176, 615(2003

78) R. E. Cohen, H. Krakauer, *Ferroelectrics*, 136, 65(1992).

79) P.G. Harrison, *Coord. Chem. Rev.*, 20, 1(1976).

80) P.G. Harrison, Silicon, Germanium, Tin and Lead (in: R.D. Gillard, J.A. McCleverty (Eds.), Sir G. Wilkinson (Editor-in-Chief), *Comprehensive Coordination Chemistry*, vol. 3), Pergamon Press, 183 (1987).

81) C. E. Holloway, M. Melnik, *Main Group Met. Chem*., 20, 399(1997).

82) C. E. Holloway, M. Melnik, *Main Group Met. Chem*., 20, 573(1997).

83) C. E. Holloway, M. Melnik, *Main Group Met. Chem.*, 20, 107(1997).

84) J. Parr, *Polyhedron* 16, 551(1997).

85) J. Parr, Germanium, Tin, and Lead (in: G. F. Parkin (Ed.), J .A. McCleverty, T.J. Meyer (Editors-in-Chief), *Comprehensive Coordination Chemistry II*, vol. 3), Elsevier, 545(2003).

86) R.L. Davidovich, Koord. Khim. 31 (2005) 483; R.L. Davidovich, *Russ. J. Coord. Chem*., 31, 455(2005).

87) R. L. Davidovicha,, Vitalie Stavila b, D. V. Marinina, E. I. Voita, K. H. Whitmirec, *Coord. Chem. Rev*., 253, 1316 (2009).

88) R. L. Davidovicha,, Vitalie Stavila b, K. H. Whitmirec, *Coord. Chem*., Rev. 254, 2193 (2010).

89) L. Shimoni-Livny, J.P. Glusker, C.W. Bock, *Inorg. Chem.*, 37, 1853(1998).

90) R.J. Gillespie, R.S. Nyholm, Quart. Rev., *Chem. Soc*., 11, 339(1957).

91) J. C. Mattos, A. M. Nunes, A. F. Martins, V. L. Dressler, É. M. Flores, *Spectrochim Acta B; Atomic Spectroscopy*, 60, 687 (2005).

92) T D. Palmer, M. E. Lewis Jr., C. M. Geraghty, F. B. Jr., P. J. Parsons. *Spectrochimica Acta Part B: Atomic Spectroscopy*, 61, 980 (2006).

93) S. Baytak, A. Rehber Türker. *J. Hazard. Mater*., 129, 130 (2006).

94) M. Vilar, J. Barciela, S. García-Martín, R.M. Peña, C. Herrero. *Talanta,* 71,1629 (2007).

95) L. F. Rodrigues, J. C. Mattos, V. L. Dressler, D. Pozebon, É. M. Flores, *Spectrochimica Acta Part B: Atomic Spectroscopy*, 62, 933 (2007).

96) A. N. Anthemidis, S. V. Koussoroplis, *Talanta*, 71, 1728 (2007).

97) T. A. Maranhão, E. Martendal, D. L.G. Borges, E. Carasek, B. Welz, A. J. Curtius, *Spectrochimica Acta Part B: Atomic Spectroscopy*, 62, 1019 (2007).

98) J. Cao, P. Liang, R. Liu, *J. Hazard. Mater*., 152, 910 (2008).

99) R. Liu, P. Liang, *J Hazard Mater*., 152, 166 (2008).

100) H. F. Maltez, D. L.G. Borges, E. Carasek, B. Welz, A. J. Curtius, *Talanta*, 74, 800 (2008).

101) M. B. Dessuy, M. G. R. Vale, A. S. Souza, S. L.C. Ferreira, B. Welz, D. A. Katskov, *Talanta*, 74, 1321(2008).

102) A. Baysal, S. Akman, F. Calisir, *J. Hazard. Mater*., 158, 454 (2008).

103) J. L. Manzoori, M. Amjadi, J. Abulhassani, *Anal. Chim. Acta*, 644, 48 (2009).

104) I. C.F. Damin, M. B. Dessuy, T. S. Castilhos, M. M. Silva, M. G. R. Vale, B. Welz, D. A. Katskov, *Spectrochimica Acta Part B: Atomic Spectroscopy*, 64, 530 (2009).

105) H. Parham, N. Pourreza, N. Rahbar, *J. Hazard. Mater*., 163, 588 (2009).

106) G. Yang, W. Fen, C. Lei, W. Xiao, H. Sun, *J. Hazard. Mater*., 162, 44 (2009).

107) C. Zeng, X. Wen, Z. Tan, P. Cai, X. Hou, *Microchem J.*, 96, 238-242(2010).

108) J. Abulhassani, J. L. Manzoori, M. Amjadi, *J. Hazard. Mater*., 176, 481 (2010).

109) A. N. Anthemidis, K. G. Ioannou, *Anal. Chim. Acta*, 668, 35 (2010).

110) K. Shrivas, D. K. Patel, *J. Hazard. Mater*., 176, 414 (2010).

111) R. J. Cassella, D. M. Brum, C. F. Lima, T. C. O. Fonseca, *Fuel Sci Techn Int.*, *92*, *933* (2011).

112) M. S. Bispo, M. A. Korn, E. S. Morte, L. S. G. Teixeira, *Spectrochimica Acta Part B: Atomic Spectroscopy*, 57, 2175 (2002).

113) K. Jankowski, J. Yao, K. Kasiura, A. Jackowska, A. Sieradzka, *Spectrochimica Acta Part B: Atomic Spectroscopy*, 60, 369 (2005).

114) Y. Xu, J. Zhou, G. Wang, J. Zhou, G. Tao, *Anal. Chim. Acta*, 584, 204 (2007).

[115] E. R. Yourd, J. F. Tyson, R. D. Koons, *Spectrochimica Acta Part B: Atomic Spectroscopy*, 56, 1731(2001).

116) L. F. Dias, T. D. Saint'Pierre, S. M. Maia, M. A. M. da Silva, V. L.A. Frescura, B. Welz, A. J. Curtius, *Spectrochimica Acta Part B: Atomic Spectroscopy*, 57, 2003 (2002).

117) E. Skrzydlewska, M. Balcerzak, F. Vanhaecke, *Anal. Chim. Acta*, 479, 191 (2003).

118) H. Hsieh, W. Chang, Y. Hsieh, C. Wang, *Talanta*, 79, 183 (2009).

119) Z. Huang, C. Yang, Z. Zhuang, X. Wang, F. S. C. Lee, *Anal. Chim. Acta*, 509, 77 (2004).

120) T. D. Saint'Pierre, L. F. Dias, S. M. Maia, *Spectrochimica Acta PartB: AtomicSpectroscopy*, 59, 551 (2004).

121) L. F. Dias, G. R. Miranda, T, D. Saint'Pierre, S. M. Maia, V. L.A. Frescura, A. J. Curtius, *Spectrochimica Acta Part B: Atomic Spectroscopy*, 60, 117 (2005).

122) A.B. Volynsky, M.T.C. de Loos-Vollebregt, *Spectrochimica Acta Part B:Atomic Spectroscopy*, 60, 1432 (2005).

123) P. K. Petrov, G. Wibetoe, D. L. Tsalev, *Spectro chimica Acta Part B:Atomic Spectroscopy*, 61, 50 (2006).

124) C. D. Palmer, M. E. Lewis Jr., C, M. Geraghty, F. Barbosa Jr., P. J. Parsons, *Spectrochimica Acta Part B: Atomic Spectroscopy*, 61, 980 (2006).

125) L. Jin, Q. Shuai, J. Jiang, S. Hu, H. Zhang, *Chinese J. Anal. Chem.*, 35, 191 (2007).

126 Y. Xu, J. Zhou, G. Wang, J. Zhou, G. Tao, *Anal. Chim. Acta*, 584, 204 (2007).

127) W. J. McShane, R. S. Pappas, V. W. McElprang, D. Paschal, *Spectrochimica Acta Part B: Atomic Spectroscopy*, 63, 638 (2008).

128) M. G. Minnich, D. C. Miller, P. J. Parsons, *Spectrochimica Acta Part B: Atomic Spectroscopy*,63, 389 (2008).

129) J. O. Romaní, A. M. Piñeiro, P. B. Barrera, A. M. Esteban, *Talanta*, 79, 723 (2009).

130) G. Grindlay, J. Mora, L. Gras, M.T.C. de L. Vollebregt, *Anal. Chim. Acta*, 652, 154 (2009).

131) S. D'Ilio, F. Petrucci, M. D'Amato, M. Di Gregorio, O. Senofonte, *Anal. Chim. Acta*, 624, 59 (2008).

132) M. Resano, M.P. Marzo, R. Alloza, C. Saénz, F. Vanhaecke, L. Yang, S. Willie, *Anal. Chim. Acta*, 677, 55 (2010).

133) F. A. Aydin, M. Soylak, *J Hazard Mater*.,173, 669 (2010).

134) J. C. Lam, K. Chan, Y. Yip, W. Tong, D. W. Sin, Food Chem., 121, 552 (2010).

135) Y. Bonfil, M. Brand, E. K. Eisner, *Anal. Chim. Acta*, 464, 99-114(2002).

136) M. E. Abdelsalam, G. Denuault, S. Daniele,. *Anal. Chim. Acta*, 452, 65-75(2002).

137) R. A. A. Munoz, L. Angnes, *Microchem J.*, 77, 157 (2004).

138) M. Panigati, M. Piccone, G. D'Alfonso, M. Orioli, M. Carin, *Talanta*, 58, 481 (2002).

139) Y. Bonfil, E. Kirowa-Eisner, *Anal. Chim. Acta*, 457, 285 (2002).

140) D. Demetriades, A. Economou, A. Voulgaropoulos, *Anal. Chim. Acta*, 519, 167 (2004).

141) J. A. Bortoloti, R. E. Bruns, J. C. de Andrade, R. K. Vieira, *Chemometr Intell Lab.*, 70, 113 (2004).

142) E. Shams, H. Abdollahi, M. Yekehtaz, R. Hajian, *Talanta*, 63, 359 (2004).

143) A. Charalambous, A. Economou,. *Anal. Chim. Acta*, 547, 53 (2005).

144) M. C. V. Mamani, L. M. Aleixo, M. F. de Abreu, S. Rath, *J. Pharm. Biomed. Anal*., 37, 709 (2005).

145) D. Dragoe, N. Spătaru, R. Kawasaki, A. Manivannan, T. Spătaru, D. A. Tryk, A. Fujishima, *ElectrochimicaActa*, 51, 2437 (2006).

146) G. Li, Z. Ji, K. Wu, *Anal. Chim. Acta*, 577, 178 (2006).

147) B.S. Sherigara, Y. Shivaraj, R. J. Mascarenhas, A.K. Satpati, *Electrochimica Acta*, 52, 3137 (2007).

148) B. Baś, M. Jakubowska, *Anal. Chim. Acta*, 615, 39 (2008).

149) Y. Wu, N. B. Li, H. Q. Luo, *Sens. Actuators, B*, 133, 677 (2008).

150) J. Jakmunee, J. Junsomboon, *Talanta*, 77, 172 (2008).

151) V. Meucci, S. Laschi, M. Minunni, C. Pretti, L. Intorre, G. Soldani, M. Mascini,. *Talanta*, 77, 1143 (2009).

152) Y. Li, X. Liu, X. Zeng, Y. Liu, X. Liu, W. Wei, S. Luo, *Sens. Actuators, B,* 139, 604 (2009).

153) Y. Wang, Z, Liu, X, Hu, J, Cao, F. Wang, Q. Xu, C. Yang, *Talanta*, 77, 1203 (2009).

154) K. C. Armstrong, C. E. Tatum, R. N. D. Sparks, J. Q. Chambers, Z. Xue, *Talanta*, 82, 675 (2010).

155) D. Li, J. Jia, J. Wang, *Talanta*, 83, 332 (2010).

156) Z. Es'haghi, M. Khalili, A. Khazaeifar, G. H. Rounaghi, *Electrochimica Acta*, *56*, *3139* (2011).

157) H. Mongi, A. Kida, N. Uchida, K. Iwasa, S. Nakano, *Microchem. J.*, 97, 220 (2011).

158) S. Saito, N. Danzaka, S. Hoshi, *J. Chromatogr B.*,1104, 140 (2006).

159) Tang, Y.; Zhai, Y.F.; Xiang, J.J.; Wang, H.; Liu, B.; Guo, *Environ. Pollut. 158*, 2074 (2010).

160) M. O. Luconi, R. A. Olsina, L. P. Fernandez, M. F. Silva, *J. Hazard. Mate. B 128*, 240 (2006).

161) Z. Yanaz, H. Filik, R. Apak, *Sens. Actuat. B147*, 15 (2010).

162) H. L. Zhang, Y. K. Ye, B. Xu, *Chin. J. Anal. Chem, 28*, 194 (2000).

163) S. Saito, N. Danzaka, S. Hoshi, *J. Chromatogr. A 1104*, 140 (2006).

164) Z. J. Huang, G. Y. Yang, Q. F. Hu, J. Y. Yin, *Anal. Sci., 19*, 255 (2003).

165) V. S. Bhat, V. S. Ijeri, A. K. Srivastava, *Sens. Actuators, B.*, 99, 98 (2004)

166) M. M. Ardakani, M. K. Kashani, M. S. Niasari, A. A. Ensafi, *Sens. Actuators, B*, 107, 438 (2005).

167) T. Jeong, H. K. Lee, D. C. Jeong, S. Jeon, *Talanta* 65, 543 (2005).

168) V. K. Gupta , A. K. Jain, P. Kumar, *Sens. Actuators, B.*, 120, 259 (2006)

169) A. K. Jain, V. K. Gupta, L. P. Singh, J. R. Raisoni, *Electrochimica Acta* 51, 2547 (2006).

170) L. Chen, J. Zhang, W. Zhao, X. He, Y. Liu, *J. Electroanal. Chem.*, 589, 106 (2006).

171) H. M. Rong, R. X. Wu, L. X. Gui, *Chinese J. Anal. Chem.*, 36, (2008).

172) S. Y. Kazemi, M. Shamsipur, H. Sharghi, *J. Hazard. Mater., 172*, 68 (2009).

173) A. Michalska, M. Wojciechowski, E. Bulska, J. Mieczkowski, K. Maksymiuk, *Talanta* 79, 1247 (2009).

174) D. Wilson, M. d. Arada, S. Alegret, M. d. Valle, *J. Hazard. Mater*., 181, 140 (2010).

175) X. G. Li, X. L. Ma, M. R. Huang, *Talanta*, 78, 498 (2009).

176) A. S. Alasier, S. A. Entisar, H. A. Elbishti, *Arabian Journal of Chemistry*, 3, 89 (2010).

177) A. Abbaspour, E. Mirahmadi, A. Khalafi-nejad, S. Babamohammadi, *J. Hazard. Mater*., 174, 656 (2010).

178) M. R. Ganjali, N. M. Kazami, F. Faridbod, S. Khoee, P. Norouzi, *J. Hazard. Mater.*, 173, 415 (2010).

179) Ion, A. Culetu, J. Costa, C. Luca, C. Alina, *Desalination*, 259, 38 (2010).

180) P. Chooto, P. Wararatananurak, C. Innuphat, *ScienceAsia,* 36, 150 (2010).

181) N. Ding, Q. Cao, H. Zhao, Y. Yang, L. Zeng, Y. He, K. Xiang and G. Wang, *Sensors*, 10, (2010).

182) M. H. Mashhadizadeh, M. Talakesh, M. Peste, A. Momeni, H. Hamidian, M. Mazlum, Electroanal., 18, 2174 (2006).

183) S. M. Saadeh, *Arabian Journal of Chemistry*., In press (2010).

184) A. M. Awadallah, and N. M. El-Halabi, *Islamic University Journal (series of Natural sciences and Engineering)* 13, 85 – 90(2005).

185) G. A. E. Mostafa, *Talanta*, 71, 1449-1454(2007).

186) S. R. Patil, N. U. Kantak, N. D. Sen, *Inorg. Chim. Acta.*, 63, 261(1982).

187) K. Dey, D. Bandyopadhyay, *Trans Metal Chem*., 16, 267(1991).

188) M. Yongxiang, Z. Zhengzhi, M. Yun, Z. Gang, *Inorg. Chim. Acta.,* 165,185(1989).

189) N. Turan, M. Sederci, *Heteroatom Chem*., 21, 14–23(2010).

190) Z. Hong-Yun, C. Dong-Li, C. Pei-Kun, C. De-Ji, C. Guang-Xia, Z. Hong-Quan, *Polyhedron,* 11, 2313(1992).

191) B. K. Singh, A. Prakash, H. Rajour, N. Bhojak, D. Adhikari, *Spectrochimica Acta*, Part A, *76*, *376-383*(2010).

192) Y. J. Jang, U. Lee, B. K. Koo, *Bull. Korean Chem. Soc*., 26, 925(2005).

193) V. S. Bhat, V. S. Ijeri, A. K. Srivastava, *Sens. Actuators*, B 99, 98–105(2004).

194) M. Shamsipur, M. Hosseini, K. Alizadeh, M. M. Eskandari, H. Sharghi, M. F. Mousavi, M. R. Ganjali, *Anal. Chim. Acta.*, 486, 93 (2003).

195) H. M. Abu-Shawish, S. M. Saadeh, A. R. Hussien, *Talanta*, 76, 941 (2008).

196) E. A. Cummings, P. Mailley, S. Linquette-Mailley, B. R. Eggins, E. T. McAdams, S. McFadden, *Analyst*, 123, 1975(1998).

197) J. S´anchez, M. Valle, *Crit. Rev. Anal. Chem*., 35, 15 (2005).

198) M. A. A. Perez, L. P. Marin, J. C. Quintana, M. Y. Pedram, *Sens. Actuators,* B 89, 262(2003).

199) P. R. Buck, E. Lindner, *Pure Appl. Chem*., 66, 2527(1994).

200) A. K. Singh, S. Mehtab, *Talanta,* 74, 806(2008).

ARABIC SUMMARY

يتضح منها أتساع مدى التقدير لهذه الأقطاب.

2- تم عمل دراسة تفصيلية بغرض الوصول إلى الظروف المثالية وذلك للحصول على أفضل استجابة لهذه الأقطاب، **detection limit were 3.9 x 10^{-7} M, 7.9 x 10^{-7} M .**

3- **لوحظ أن الاستجابة الجهدية للأقطاب لا تتأثر بالأس الهيدروجيني في المدى pH range 6.2-7.8**

4- أظهرت دراسة تأثير درجة الحرارة على الاستجابة الجهدية للأقطاب أنها تتميز بثبات حراري كبير في المدى 20-50 درجة سليزيوس.

6- وجد أن زمن الاستجابة الجهدية للأقطاب يتراوح بين 8 - 10 ثانية فقط.

7- كان تقدير الرصاص التي تحت الدراسة باستخدام الأقطاب المحضرة في عينات مختلفة بطريقة الإضافات القياسية و أيضا المعايرة الجهدية و استخدام المنحنى العياري على درجة عالية من الدقة و الحساسية.

8- مع تحليل النتائج إحصائيا وجد أن هناك تطابق بين الطرق المستخدمة مع الطرق الأخرى وهذا يدل على مدى دقة الطرق المطبقة.

بسم الله الرحمن الرحيم

Synthesis and characterization of lead(II) complexes with some polydentate ligands and their application in lead(II)-selective electrodes

تحضير ودراسة معقدات الرصاص(II) مع بعض المتصلات عديدة السّن واستعمالها مجسّات للرصاص(II)

تصف الرسالة تحضير مركبات جديدة من معقدات الرصاص(II) مع بعض المتصلات عديدة السّن تحتوى على ثلاث ذرات مانحة مثل ONO وSNO ، والصيغة العامة لهذه المعقدات PbL_2، حيث L هو الأيون السالب لهذه المتصلات.
هذه المتصلات عديدة السن عبارة عن: 2- اسيتيل ثيوفين بنزويل هيدرازون (ATBH)، 2- اسيتيل فيورين بنزويل هيدرازون (AFBH) ، 2- كاربوكسالدهيد ثيوفين بنزويل هيدرازون (CTBH)، 2- كاربوكسالدهيد فيورين بنزويل هيدرازون (CFBH).
وحضرت هذه المعقدات من تفاعل اسيتات الرصاص (II) مع كل واحدة من هذه المتصلات فى الميثانول بنسبة 1 : 2.
هذه المعقدات لا تذوب فى المذيبات العضوية الشائعة لكنها تذوب فى DMF و DMSO
عند قياس التوصيلية المولية (molar conductance values) تبين أن هذه المعقدات ليست الكتروليتية (non electrolytes in nature) .
تم تميزهذه المعقدات باستخدام التحليل العنصرى وأجهزة مطيافية المنطقة فوق البنفسجية، مطيافية تحت الحمراء، ومطيافية الرنين النووى المغناطيسى، وجد أن الذرة المركزية (الرصاص(II)) فى المعقدات يمتلك شكله ثمانى السطوح حيث فيها المتصلات عديدة السن ترتبط مع الرصاص(II) من خلال النيتروجين (أزوميثن)، والأكسجين (بنزويل)، والكبريت (ثيوفين) أو الأكسجين (الفيورين).
وقد استعملت هذه المعقدات فى تحضير أقطاب انتقائية من عجينة الكربون لتقدير الرصاص فى الماء (كمجسات للرصاص (II)).
المعقد $Pb(ATBH)_2$ أعطى أفضل استجابة مع اثنين من الملدنات (**DOS**) **و** (TEph)**.**
تم دراسة العديد من العوامل التي يتوقع أن يكون لها تأثير على فاعلية هذه الأقطاب مثل درجة الحرارة و زمن الاستجابة و التكرارية والأس الهيدروجيني. وتم استخدام طريقة الإضافات القياسية و المعايرة الجهدية و المنحنى العياري فى تحديد خواص الأقطاب.

استخدام هذه الأقطاب نوقشت في النقاط التالية:

1- مدى التركيزات التي تم تقديرها بهذه الأقطاب كانت

$5.9 \times 10^{-7} - 1.0 \times 10^{-2}$ M, 9.1×10^{-7} -1.0 x 10^{-2} M

الملخص بالعربى

بسم الله الرحمن الرحيم

(قالوا سبحانك لا علم لنا إلا ما علمتنا
انك أنت العليم الحكيم)

(البقرة : 32)

صدق الله العظيم

الجامعة الاسلامية – غزة

عمادة الدراسات العليا

كلية العلوم – قسم الكيمياء

تحضير ودراسة معقدات الرصاص(II) مع بعض المتصلات عديدة السّن واستعمالها مجسّات للرصاص(II)

رسالة مقدمة من /

بهاء الدين خضر عايد ضاهر

المشرفان

الدكتور سلمان مصطفى سعادة
أستاذ مشارك
الجامعة الإسلامية – غزة

الدكتور حازم محمد أبو شاويش
أستاذ مشارك
جامعة الأقصى - غزة

قدمت كجزء من المتطلبات اللازمة لنيل درجة الماجستير في الكيمياء

قسم الكيمياء– كلية العلوم

الجامعة الاسلامية – غزة

غزة – فلسطين

1432هـ - 2011م